pancreas. *Am J Physiol Gastrointest Liver Physiol* 277: G487–G494, 1999.
28. **Montrose MH and Murer H.** Regulation of intracellular pH by cultured opossum kidney cells. *Am J Physiol Cell Physiol* 259: C110–C120, 1990.
29. **Muallem S and Loessberg PA.** Intracellular pH-regulatory mechanisms in pancreatic acinar cells. I. Characterization of H^+ and HCO_3^- transporters. *J Biol Chem* 265: 12806–12812, 1990.
30. **Noone PG, Zhou Z, Silverman LM, Jowell PS, Knowles MR, and Cohn JA.** Cystic fibrosis gene mutations and pancreatitis risk: relation to epithelial ion transport and trypsin inhibitor gene mutations. *Gastroenterology* 121: 1310–1319, 2001.
31. **Novak I and Greger R.** Electrophysiological study of transport systems in isolated perfused pancreatic ducts: properties of the basolateral membrane. *Pflügers Arch* 411: 58–68, 1988.
32. **Romero MF, Hediger MA, Boulpaep EL, and Boron WF.** Expression cloning and characterization of a renal electrogenic Na^+/HCO_3^- cotransporter. *Nature* 387: 409–413, 1997.
33. **Roussa E, Romero MF, Schmitt BM, Boron WF, Alper SL, and Thevenod F.** Immunolocalization of anion exchanger AE2 and Na^+-HCO_3^- cotransporter in rat parotid and submandibular glands. *Am J Physiol Gastrointest Liver Physiol* 277: G1288–G1296, 1999.
34. **Scheele GA, Fukuoka SI, Kern HF, and Freedman SD.** Pancreatic dysfunction in cystic fibrosis occurs as a result of impairments in luminal pH, apical trafficking of zymogen granule membranes, and solubilization of secretory enzymes. *Pancreas* 12: 1–9, 1996.
35. **Schmitt BM, Berger UV, Douglas RM, Bevensee MO, Hediger MA, Haddad GG, and Boron WF.** Na/HCO_3^- cotransporters in rat brain: expression in glia, neurons, and choroid plexus. *J Neurosci* 20: 6839–6848, 2000.
36. **Seki G, Coppola S, and Frömter E.** The Na^+-HCO_3^- cotransporter operates with a coupling ratio of 2 HCO_3^- to 1 Na^+ in isolated rabbit renal proximal tubule. *Pflügers Arch* 425: 409–416, 1993.
37. **Shumaker H, Amlal H, Frizzell R, Ulrich CD, 2nd, and Soleimani M.** CFTR drives Na^+-HCO_3^- cotransport in pancreatic duct cells: a basis for defective HCO_3^- secretion in CF. *Am J Physiol Cell Physiol* 276: C16–C25, 1999.
38. **Thévenod F, Roussa E, Schmitt BM, and Romero MF.** Cloning and immunolocalization of a rat pancreatic Na^+ bicarbonate cotransporter. *Biochem Biophys Res Commun* 264: 291–298, 1999.
39. **Thomas JA, Buchsbaum RN, Zimniak A, and Racker E.** Intracellular pH measurements in Ehrlich ascites tumor cells utilizing spectroscopic probes generated in situ. *Biochemistry* 18: 2210–2218, 1979.
40. **Usui T, Hara M, Satoh H, Moriyama N, Kagaya H, Amano S, Oshika T, Ishii Y, Ibaraki N, Hara C, Kunimi M, Noiri E, Tsukamoto K, Inatomi J, Kawakami H, Endou H, Igarashi T, Goto A, Fujita T, Araie M, and Seki G.** Molecular basis of ocular abnormalities associated with proximal renal tubular acidosis. *J Clin Invest* 108: 107–115, 2001.
41. **Usui T, Seki G, Amano S, Oshika T, Miyata K, Kunimi M, Taniguchi S, Uwatoko S, Fujita T, and Araie M.** Functional and molecular evidence for Na^+-HCO_3^- cotransporter in human corneal endothelial cells. *Pflügers Arch* 438: 458–462, 1999.
42. **Yoshitomi K, Burckhardt BC, and Frömter E.** Rheogenic sodium-bicarbonate cotransport in the peritubular cell membrane of rat renal proximal tubule. *Pflügers Arch* 405: 360–366, 1985.
43. **Zhao H, Star RA, and Muallem S.** Membrane localization of H^+ and HCO_3^- transporters in the rat pancreatic duct. *J Gen Physiol* 104: 57–85, 1994.

ACADEMIC PRESS

Available online at www.sciencedirect.com

SCIENCE DIRECT®

Virology 317 (2003) 24–35

VIROLOGY

www.elsevier.com/locate/yviro

Antiapoptotic regulation by hepatitis C virus core protein through up-regulation of inhibitor of caspase-activated DNase

Rodolfo Sacco,[a,1] Takeya Tsutsumi,[a,b] Ryosuke Suzuki,[a] Motoyuki Otsuka,[c] Hideki Aizaki,[a,2] Shinichiro Sakamoto,[a] Mami Matsuda,[a] Naohiko Seki,[d] Yoshiharu Matsuura,[e] Tatsuo Miyamura,[a] and Tetsuro Suzuki[a,*]

[a] *Department of Virology II, National Institute of Infectious Diseases, Tokyo, Japan*
[b] *Department of Internal Medicine, Graduate School of Medicine, University of Tokyo, Tokyo, Japan*
[c] *Department of Gastroenterology, Graduate School of Medicine, University of Tokyo, Tokyo, Japan*
[d] *Department of Functional Genomics, Graduate School of Medicine, Chiba University, Chiba, Japan*
[e] *Research Center for Emerging Infectious Diseases, Research Institute for Microbial Diseases, Osaka University, Osaka, Japan*

Received 10 March 2003; returned to author for revision 7 August 2003; accepted 19 August 2003

Abstract

The hepatitis C virus (HCV) core protein is considered to influence multiple cellular processes. We developed a human hepatoblastoma HepG2-derived inducible cell line, Hep191, which allows tightly regulated expression of the core protein at relatively low but physiological levels under control of the ecdysone-regulated promoter. By transcriptional profiling, we identified differentially expressed genes, some of which are involved in cell growth or apoptosis such as inhibitor of caspase-activated DNase (ICAD), defender against cell death 1, tumor necrosis factor (TNF) receptor 1, and cytochrome c oxidase subunit VIII. Furthermore, we found that core protein expression increases a steady-state level of ICAD protein, possibly through enhancing its promoter activity, and inhibits caspase-3 activity induced by anti-Fas antibody. Since Fas- or TNF-mediated DNA fragmentation is suppressed in the core-induced Hep191 cells, these findings suggest that expression of HCV core at physiological levels confers blocking activity of caspase-activated DNase and consequently inhibiting apoptotic cell death.

Keywords: Hepatitis C virus; Microarray; DNA fragmentation; Apoptosis; Caspase-3

Introduction

A main characteristic feature of hepatitis C virus (HCV) infection is its persistent nature, which often leads to chronic hepatitis and liver cirrhosis. HCV infection is also strongly associated with the development of hepatocellular carcinoma (HCC) (Choo et al., 1989; Kuo et al., 1989; Saito et al., 1990). Another characteristic is its highly specific host range for replication. To understand the exact mechanism of pathogenesis and persistence of HCV infection, it is important to elucidate virus–cell interaction, particularly in hepatic cells. We have been interested in the role of HCV core protein, which constitutes not only viral nucleocapsids but has multifunctions for pathogenesis or establishment of persistent infection of HCV (Lai and Ware, 1999; Thomson and Liang, 2000; Suzuki et al., 1999).

Apoptosis is definitely one of the key factors associated with liver injury and chronicity of HCV infection (Hayashi and Mita, 1997; Lau et al., 1998; Patel et al., 1998). However, its molecular mechanism is not clear yet. Apoptosis mediated by Fas or tumor necrosis factor (TNF) is a major pathway involved in a wide range of liver diseases. When

* Corresponding author. Department of Virology II, National Institute of Infectious Diseases, 1-23-1 Toyama, Shinjuku-ku, Tokyo 162-8640, Japan. Fax: +81-3-5285-1161.
E-mail address: tesuzuki@nih.go.jp (T. Suzuki).
[1] Present address: Gastroenterology and Hepatology Unit, Pisa University Hospital, Pisa, Italy.
[2] Present address: Department of Microbiology, University of Southern California, Los Angeles, CA, USA.

0042-6822/$ – see front matter © 2003 Elsevier Inc. All rights reserved.
doi:10.1016/j.virol.2003.08.028

Fas is constitutively expressed in hepatocytes and when agonistic anti-Fas antibodies are injected, the animals develop fatal fulminant hepatitis (Ogasawara et al., 1993; Lacronique et al., 1996). On the other hand, several HCV proteins have been reported to modulate apoptosis induced by diverse stimuli in different experimental systems (Ray et al., 1996, 1998; Fujita et al., 1996; Ruggieri et al., 1997; Zhu et al., 1998, 2001; Marusawa et al., 1999; Dumoulin et al., 1999; Gale et al., 1999; Hahn et al., 2000; Tai et al., 2000; Honda et al., 2000; Otsuka et al., 2002). However, the data shown to date, particularly with regards to the effects of the core protein, are not consistent. Several studies showed that the viral protein sensitizes apoptosis mediated by Fas, TNF-α, or other signaling pathways, whereas other studies showed inhibition of such apoptosis. Difficulty in unraveling of functions of HCV proteins on pathogenesis might be due to, at least in part, the fact that many previous investigations were based on transient or stable expression systems using unrelevantly high expression systems. In these systems, only certain populations of cells expressing viral proteins at high levels were selected. Such settings may be different from those of chronic infection, where only low production of viral proteins is observed.

In the current study, we overcame this problem through the use of the ecdysone-based inducible system, in which expression of HCV core protein can be induced at physiological levels in the same cellular background. The combination of transcriptional profiling with functional studies demonstrated the alteration of expression of several cellular genes including those related to apoptosis. It is of interest to note that expression of the core protein increased a steady-state protein level of inhibitor of caspase-activated DNase (ICAD), possibly through enhancing its promoter activity, and inhibited caspase-3 activity induced by anti-Fas antibody. In addition, induced expression of HCV core protein inhibited Fas- and TNF-mediated DNA fragmentation. These findings suggest that up-regulation of ICAD and inhibition of caspase-3 activity by the core protein collaboratively play roles in inhibiting apoptotic cell death through blocking activity of caspase-activated DNase (CAD).

Results

Establishment of a cell line allowing the tightly regulated expression of HCV core protein

The ecdysone-inducible system was used to generate tightly regulated cell lines expressing HCV core protein. This system is based on the binding of the steroid hormone ecdysone analog such as ponasterone A (PNA) to a heterodimeric receptor comprising a modified ecdysone receptor (VgEcR) and retinoid X receptor (RXR). The binding subsequently activates the ecdysone-responsive promoter to express the target genes (No et al., 1996). After keeping the transfected culture for 3 weeks in the presence of Hygromycin and Zeocin, 27 Zeocin-Hygromycin-resistant clones were isolated. They were then screened for regulated HCV core expression by sensitive fluorescence enzyme immunoassay (FEIA) and Western blot analysis. Being induced by treatment with PNA (0.3–30 μM) for 36 h, three of these clones (designated as Hep191) showed tightly regulated expression of the core protein. Western blot analysis of Hep191, clone 3 showed induction of 21-kDa HCV core protein in the presence of 30 μM PNA. It was not detected in the absence of PNA (Fig. 1A). FEIA analysis revealed that HCV core protein was observed as early as 3 h after addition of PNA and increased consistently up to 24 h. Continuous treatment with PNA showed that intracellular level of the core protein achieved after 24-h treatment was maintained during the whole culture period. Induced expression of the core protein was confirmed by indirect immunofluorescence staining (Fig. 1B). HCV core protein induced by treatment with 30 μM PNA for 48 h was localized exclusively within the cytoplasm. It seems that the core protein was essentially expressed uniformly in the induced Hep191 cells. No immunoreactivity was observed when the cells were cultured in the absence of PNA (data not shown).

We then examined "turning off" the regulation. Transcription intermediates of HCV core gene were monitored by reverse transcription-polymerase chain reaction (RT-PCR) in the cells in which the PNA medium was replaced by the vehicle-containing medium (Fig. 1C). No HCV cDNA transcript was detectable after 24 h of PNA removal. Correspondingly, HCV core protein level decreased and it was not observed after 24 h of withdrawal by Western blotting (data not shown). Further quantitative analysis by FEIA indicated that PNA's HCV core protein induction is in a concentration-dependent manner with the range of 0.3–30 μM of PNA for 36 h (Fig. 1D). No detectable level of HCV core protein was observed in the cells not treated with PNA, indicating negligible background of expression in the uninduced states. Notably, this core protein level in Hep191 is comparable to those in the livers of hepatitis C patients (6–1000 pg/mg total protein) and the transgenic mice developing hepatic steatosis and HCC (13–804 pg/mg total protein)(Koike et al., 2002; Tsutsumi et al., 2003).

Previous studies examining functional properties of HCV proteins have been performed mainly in cells overproducing the viral proteins. Moreover, many of them were nonhuman liver cells or human nonliver cells. Our human liver cell derived Hep191 cells allow the tightly regulated expression of core protein at a physiological level. This will provide a unique system to investigate possible roles of core protein in viral pathogenesis. In most of the following experiments, Hep191, clone 3 was used and core protein expression was induced by adding 10 μM PNA. Under this condition, the core protein level in the cells was approximately 500 to 1000 pg/mg total protein, which was little detected by Western blotting. We obtained similar results with the other two clones 21 and 37. These three clones

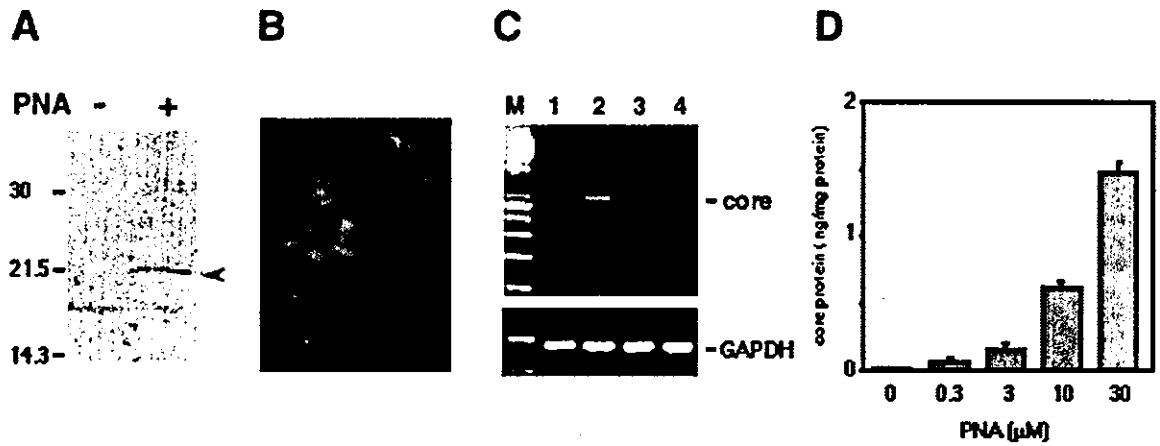

Fig. 1. Inducible expression of HCV core protein in Hep191 cells, clone 3. (A) Hep191 cells cultured in the presence (+) and absence (−) of 30 μM ponasterone A (PNA) for 36 h were analyzed by Western blotting with anticore monoclonal antibody. Arrow shows the core protein. The sizes in kDa of molecular mass markers are indicated on the left. (B) Indirect immunofluorescence staining of Hep191 cells after 48-h treatment with 30 μM PNA by monoclonal anticore antibody. (C) Tight control of the core gene expression was determined by RT-PCR. Total RNAs were isolated from Hep191 cells before PNA treatment (lane 1), after 24-h treatment (lane 2). Subsequently, the treated cells were washed, followed by another culture in the vehicle-containing medium for 24 h (lane 3) or 48 h (lane 4). RT-PCR was performed using primers specific for genes of the core (top) and glyceraldehyde-3-phosphatase dehydrogenase (GAPDH) (bottom). Molecular size marker is shown at the left sides in both panels (M). (D) Core protein levels in Hep191 cells cultured with various concentrations of PNA for 36 h was quantified by FEIA. Data shown represent the mean values with standard deviation (S.D.) of triplicate experiments.

have been maintained in culture for over 20 months and more than 90 passages without loss of tightly regulated gene expression.

Cell growth properties

To test the effects of induced expression of HCV core protein on cell growth, Hep191 cells were cultured in daily changed medium with or without PNA. The number of viable cells was determined by counting daily for 10 days. As shown in Fig. 2A, no differences were noted between growth curves of Hep191 cultured in the medium with 10% fetal bovine serum (FBS) in the presence and absence of PNA. Furthermore, the same saturation density was reached under both conditions. The result demonstrates that HCV core protein expressed in Hep191 cells has no influence on growth capacity, which is consistent with that in previous studies using human hepatoma Huh-7 cells (Li et al., 2002) and human osteosarcoma U-2OS cells (Moradpour et al., 1996) with tetracycline-inducible systems. Analogous results were found in slower growing Hep191 cells cultured in 1% FBS-containing medium (Fig. 2B), suggesting that core expression does not confer serum independence to the cells. We also observed that the inducing agent, PNA, exerted no pleiotropic effects, confirming the advantage of using ecdysteroids, which are known not to affect physiology of mammalian cells.

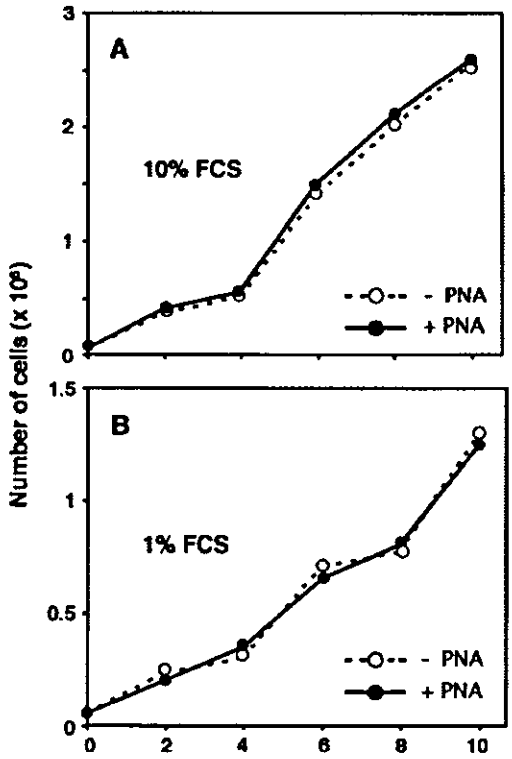

Fig. 2. Cell growth analysis. Hep191 cells were grown in the medium with 10% (A) and 1% (B) FBS in either the presence (closed circle) or the absence (open circle) of 10 μM PNA and were counted every other day as described under Materials and methods. Results show the mean cell numbers in each dish obtained from triplicate experiments.

Changes in gene expression in the core-induced Hep191 cells

We then compared the gene expression patterns in Hep191 cells in the presence and absence of 10 μM PNA.

Table 1
Genes up- or down-regulated by expression of HCV core protein in Hep191 cells

Accession no.	Gene name	Category	Fold change
AK091194	Probable trans-1,2-dihydrobenzene-1,2-dioldehydrogenase	Metabolism	2.3
Y12653	Diubiquitin	Immune response	2.2
M90657	Tumor-associated antigen L6	Tumor associated	2.2
Y12065	Nucleolar protein hNop56	RNA/protein metabolism	2.1
S54005	Thymosin beta-10	Cell motility	2.1
X74981	Keratin 8	Cell structure	2.1
M29064/M29065	Heterogeneous nuclear ribonucleoprotein A2/B1	RNA/protein metabolism	2.1
U91985	Inhibitor of caspase-activated DNase (ICAD)	Apoptosis	2.1
AH000826	Dihydrodiol dehydrogenase	Metabolism	2.1
D15057	Deffender against cell death 1, DAD1	Apoptosis	2.0
L22009	hnRNP H	RNA/protein metabolism	2.0
P05215	Tubulin alpha-4 chain	Cell structure	2.0
AF517226	Insulin-like growth factor 2 (somatomedin A)	Signaling	0.3
X54989	Evi-1	Signaling	0.4
M55422	Krueppel-related zinc finger protein, H-plk	Transcription	0.4
J04823	Cytochrome C oxidase subunit VIII-liver/heart precursor	Apoptosis	0.4
P09565	Putative insulin-like growth factor II associated protein	Signaling	0.4
M75866	TNF receptor 1	Apoptosis	0.4
BC037225	AP-2 beta (activating enhancer-binding protein 2 beta)	Transcription	0.5
U10439	Double-stranded RNA adenosine deaminase	RNA/protein metabolism	0.5

Note. Genes with two-fold or more increase (top) or decrease (bottom) in average of two experiments are indicated.

A cDNA microarray consisting of 2304 human genes was used. cDNA labeling reactions were carried out in duplicate where the fluorescent dyes, Cy3 and Cy5, were switched during the synthesis, followed by hybridizing each probe pair to a separate microarray. A list of the genes demonstrating greater than two-fold change in average of two experiments is provided in Table 1. We observed 12 genes up-regulated and 8 genes down-regulated upon induction of the core protein. Most of the genes differentially expressed were regulators of either transcription, RNA/protein metabolism, apoptosis, or signaling molecules. Among these, four genes which are involved in apoptosis regulation are noteworthy: the expression of (i) ICAD and (ii) defender against cell death 1 (DAD1) was increased, whereas the expression of (iii) TNF receptor 1 (TNFR1) and (iv) cytochrome c oxidase subunit VIII was decreased in the core-induced Hep191 cells.

To validate the differential expression of these genes, we performed semiquantitative RT-PCR analysis. For each assay, the reaction conditions and cycle numbers of PCR were individually optimized and adjusted so that the reaction fell within the linear range of product amplification. Glyceraldehyde-3-phosphatase dehydrogenase (GAPDH), whose expression was not altered, was used as a control for loading. Our RT-PCR qualitatively agreed with the expression patterns generated by microarray data (Fig. 3A). PNA itself had no effect, or little if any, on these gene expressions in control HepRXR cells, which are not expressing the core protein. In addition to analyzing clone 3 of Hep191, semiquantitative RT-PCR was also performed with ICAD and GAPDH genes of clone 37 (Fig. 3B). In good agreement with that observed with clone 3, expression of ICAD gene was up-regulated after induced expression of the core protein in clone 37.

Expression of the core protein resulted in activation of the ICAD promoter

We next focused on the impact of the core protein on ICAD expression. ICAD is a 45-kDa inhibitor of CAD, caspase-activated DNase, of 40-kDa (Liu et al., 1997; Enari et al., 1998). ICAD exists as a complex with CAD in

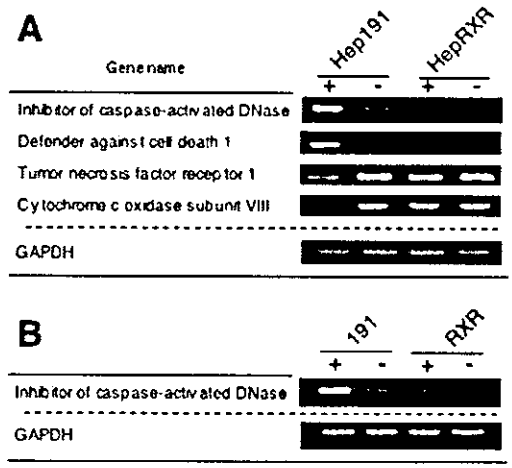

Fig. 3. Semiquantitative RT-PCR analysis of differentially expressed genes which are related to apoptosis. Total RNAs were extracted from Hep191 clone 3 (A) or clone 37 (B) and HepRXR cells cultured either with (+) or without (−) 10 μM PNA, followed by semiquantitative RT-PCR analysis. GAPDH was amplified in parallel as a control.

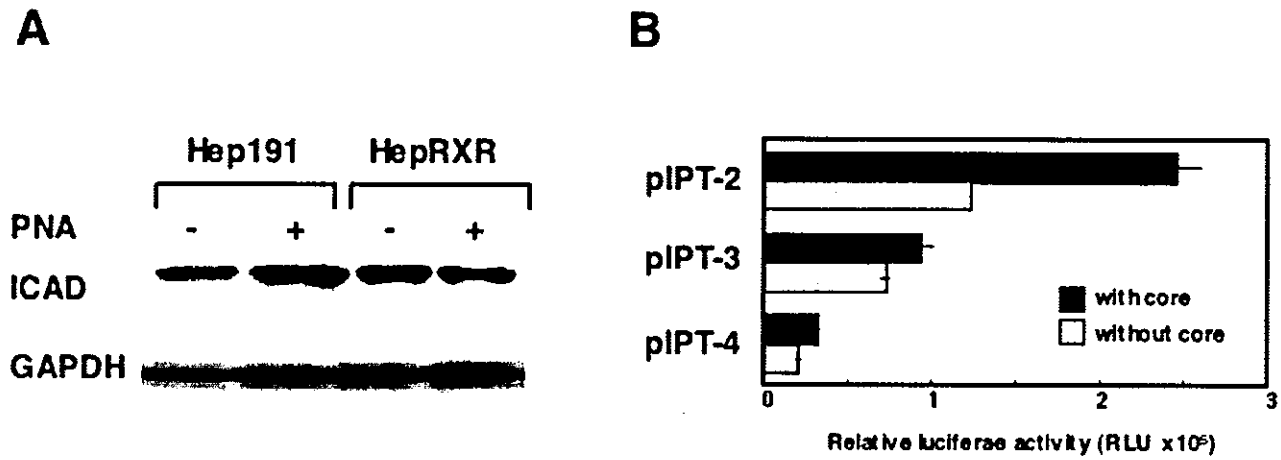

Fig. 4. Up-regulation of ICAD expression by the core protein. (A) ICAD and GAPDH expressed in Hep191 and HepRXR cells in the absence (−) or the presence (+) of PNA were analyzed by Western blotting. (B) 293T cells were cotransfected with the ICAD promoter/luciferase construct (either pIPT-2, -3, or -4) and the internal control pRL-TK in the presence of core-expressing pCAGC191 or control empty vector. Relative luciferase activity (RLU) was determined at 24 h posttransfection. Results are expressed as a mean ± S.D. of triplicate experiments.

proliferating cells. Upon apoptotic stimuli, caspases, particularly caspase-3, proteolytically process ICAD to release CAD from the complex, allowing CAD to catalyze the fragmentation of chromosomal DNA. As shown in Fig. 4A, we found a significant increase in ICAD protein in Hep191 cells treated with 10 μM PNA for 48 h by Western blotting, whereas no change was observed in the control cells with the same treatment.

To address the molecular mechanism of up-regulation of ICAD expression by core protein, we examined whether the core expression is linked to ICAD promoter activity. ICAD promoter/luciferase reporter constructs used in this study are generous gifts from Dr. S. Nagata (Kawane et al., 1999). However, HepG2-based Hep191 cells have low transfection efficiency, and these cells were not suitable for cotransfection experiments of control and experimental reporter vectors. We therefore adopted the 293T transient transfection system, in which transfection efficiency of each plasmid exhibits constantly about 80%. As shown in Fig. 4B, luciferase activity expressed from ICAD reporter construct, which includes the 110-bp 5′ flanking region of the ICAD gene (pIPT-2), increased twofold following expression of the core protein. On the other hand, the 39-bp deletion at 5′ region of the promoter (pIPT-3) resulted in a marked decrease with the core expression. The 39-bp region thus plays a role in regulating ICAD promoter activity by HCV core protein. Further 24-bp deletion (pIPT-4) caused threefold reduction of the activity in cells in both the presence and the absence of the core protein. The ICAD gene used in this reporter assay was murine in origin, but its 110-bp promoter region has 75% sequence identity to that in human ICAD gene. Furthermore, the putative binding sites for transcription factors, such as USF1 and GATA-1 in the 39-bp region, are well conserved between murine and human ICAD genes. Thus, these data indicate that stimulation of ICAD promoter activity by the core protein results in an elevated level of ICAD protein in the core-expressing cells.

Effects of HCV core protein expression on Fas- and TNF-α-mediated DNA fragmentation in Hep191 cells

The above observation showing changes in expression of several apoptosis-related genes prompted us to study the role of HCV core protein in Fas- or TNF-α-mediated apoptosis pathway. Hep191 cells with or without core induction were treated with anti-Fas antibody for 14 h. DNA ladders due to activation of nuclear endonucleases were then measured by quantitating cytoplasmic mono- and oligonucleosomes. As indicated in Fig. 5A, Hep191 cells treated with 10 μM PNA showed decreased sensitivity against anti-Fas-induced DNA fragmentation. DNA-associated mono- and oligonucleosomes released into cytoplasm were reduced to 28% in the core-expressing Hep191 cells. To exclude the direct effects of PNA in apoptotic response, we examined the Fas-induced DNA fragmentation also in the control HepRXR cells. No difference in apoptotic response was observed in HepRXR cells in either the presence or the absence of PNA (Fig. 5A). Prolonged induction of the core protein expression for 15 or 30 days with 10 μM PNA also inhibited the Fas- and TNF-α-mediated apoptosis (Fig. 5B).

We further investigated the relation of induced HCV core protein and Fas-mediated apoptotic response. As shown by the terminal deoxynucleotidyltransferase-mediated dUTP nick end-labeling (TUNEL) technique in Fig. 6, anti-Fas-treated Hep191 cells in the absence of PNA underwent apoptosis. Apoptotic cells showing DNA strand breaks were clearly demonstrated by in situ labeling. In contrast, the cells expressing HCV core protein exhibited little detectable fluorescence.

We further examined whether the induction of HCV core

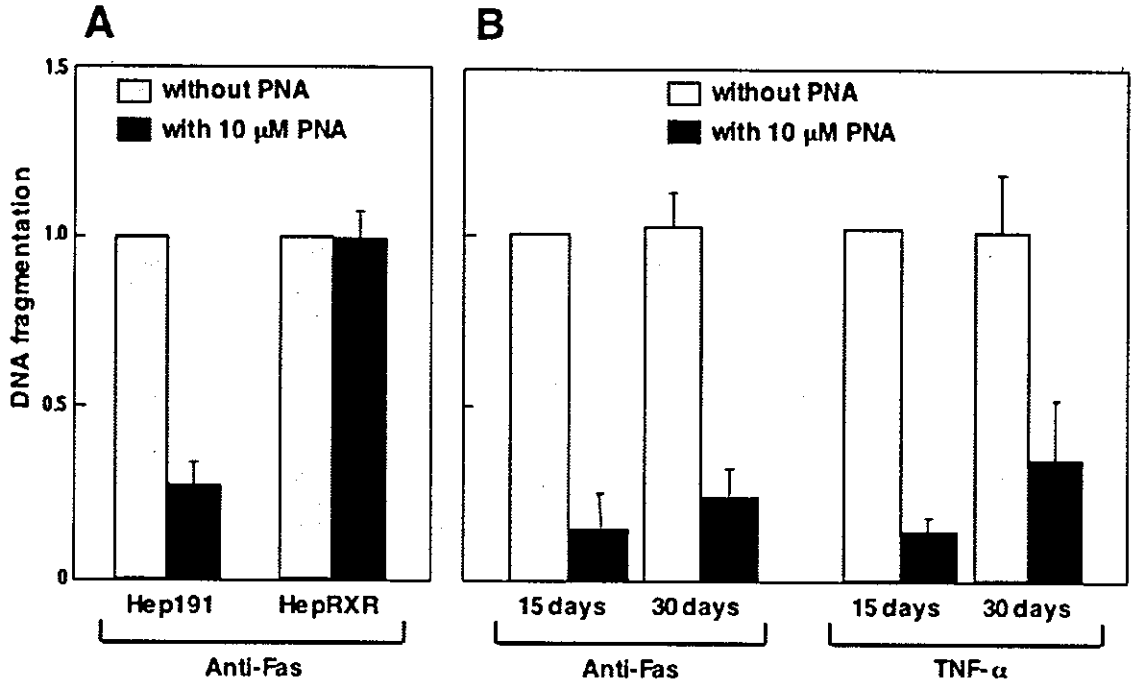

Fig. 5. Quantitation of apoptotic DNA fragmentation. (A) Hep191 and HepRXR cells, which cultured in the presence or absence of 10 μM PNA for 36 h, were treated with anti-Fas antibody and CHX for a further 14 h. Apoptotic DNA fragmentation was measured using a sandwich enzyme-linked immunosorbant assay system for cell death detection. Relative values are shown as means ± S.D. of independent three experiments. (B) Hep191 cells were grown in the presence of 10 μM PNA with repeated replacing the medium for 15 or 30 days, followed by treating with either anti-Fas/CHX for 14 h or TNF-α for 48 h.

protein would inhibit the anti-Fas-stimulated caspase-3 activity. Treatment of the core-induced Hep191 cells with anti-Fas resulted in a decrease in the caspase-3 (or DEVDase) activity in these cell lysates (Fig. 7A). Addition of PNA may not affect the enzyme activity per se, because no caspase-3 activity change was observed in HepRXR cells in the presence of 10 μM PNA. However, it is known that the treatment with anti-Fas antibody triggers the cleavage of the inactive proform of caspase-3 by an upstream caspase to generate its active subunits (Dubrez et al., 1996). Thus, we analyzed the level of 32-kDa procaspase-3, which decreases upon enzyme activation, by Western blotting (Fig. 7B). As expected, Hep191 cells without PNA treatment demonstrated a decrease in the amount of the procaspase-3 in response to anti-Fas antibody. By contrast, the level of procaspase-3 in the cells treated with 10 μM PNA was comparable to that under no apoptotic stimuli. We observed similar results in the other Hep191 clone, 37 (Fig. 7C), confirming that activation of caspase-3 following treatment with anti-Fas antibody was inhibited by induced expression of the core protein. Since caspase-3 locates almost at the end of the apoptotic cascade, its inhibition strongly indicates

Fig. 6. Photomicrographs of Hep191 cells with induced expression of the core protein. Cells were cultured in the absence (B) or presence (C) of 10 μM PNA for 36 h, followed by treating with anti-Fas antibody and CHX for a further 14 h. PNA-treated cells without inducing apoptosis by anti-Fas/CHX were also prepared (A). Apoptotic cells were visualized by TUNEL fluorescence analysis.

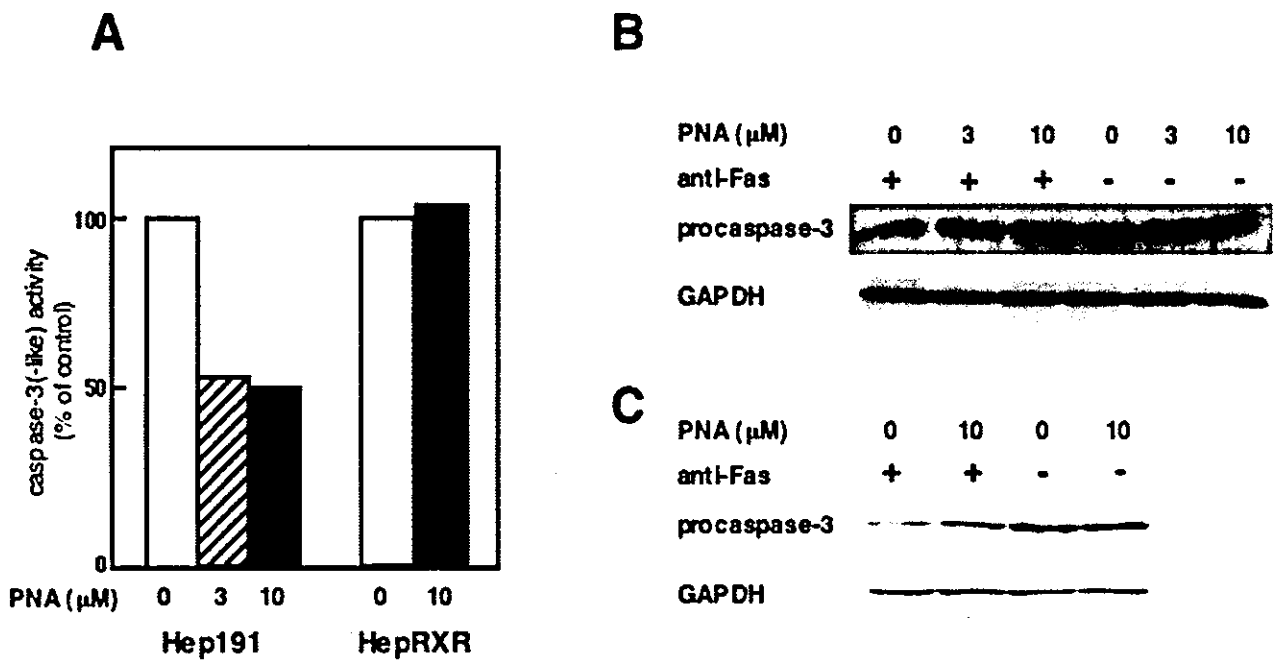

Fig. 7. Effect of the core protein on enzymatic activity and processing of caspase-3 (A) Hep191 (clone 3) and HepRXR cells grown in the presence of 0–10 μM PNA for 40 h were treated with anti-Fas/CHX, followed by measuring caspase-3 activity in cell lysates as described under Materials and methods. Results show the mean values of triplicate experiments. (B) Lysates from Hep191 cells (clone 3) cultured in the presence of 0–10 μM PNA with or without anti-Fas treatment were analyzed by Western blotting to detect procaspase-3 and GAPDH. (C) Same as in (B), but with the other Hep191 clone, 37.

that induced expression of the HCV core protein at moderate levels inhibits Fas-mediated DNA fragmentation in human liver cells.

Discussion

Deregulation of apoptosis or programmed cell death is involved in a wide range of pathological processes, including autoimmune hepatitis, fulminant hepatitis, and HCC. Although there is increasing evidence that the HCV core protein interacts with regulatory pathways controlling apoptosis, the role of this protein remains controversial because of the conflicting results in the literature, that is, its opposite effects in either inhibition or potentiation of apoptosis. It is likely that the expression level of the core protein, availability of apoptotic versus survival factors, and experimental setting might affect the fate of cells exposed to diverse stimuli.

In the current study, we have introduced the ecdysone-inducible expression system to establish a human hepatoblastoma HepG2-based stable cell line, Hep191, allowing tightly regulated expression of HCV core protein. In this system, no background expression is observed in the absence of the inducer. It is also possible to precisely control the expression levels in response to varying inducer concentrations. These are the advantages of using the ecdysone-based system over other inducible systems, such as the tetracycline-based system. Indeed, the ecdysone-inducible system was developed to address a main flaw of the tetracycline-inducible system, a relatively high background of expression in the uninduced state (No et al., 1996). In contrast to tetracycline, the lipophilic nature of the ecdysteroids such as PNA allows their efficient penetrance into cells and appropriate pharmacokinetics that prevent storage and expedite clearance, leading to a delicate temporal control of gene expression. Further, we observed no pleiotropic effects of the inducing agent. Neither cytotoxicity nor influence on cell proliferation was observed in PNA-treated cells (Fig. 2). The lack of baseline cross-talk between the inducible system and endogenous cellular pathway is essential to study HCV–liver cell interaction. It is also noteworthy that the expression levels of HCV core protein in Hep191 cells can be controlled to the level comparable to those in the livers of hepatitis C patients and the HCV core-transgenic mice developing hepatic steatosis and HCC (Koike et al., 2002; Tsutsumi et al., 2003). In this regard, most of the previous studies on possible roles of HCV core protein in viral pathogenesis depended on overexpression systems of either constitutively expressing cell lines or transiently transfected cells. Thus, Hep191 cells based on the ecdyson system may be useful as a model of HCV core–host cell interaction closer to the virus infection setting than previous expression systems. Liver cell specific interaction included in this system would be important.

We applied this Hep191 cell line to analyze the gene

expression profiling by using cDNA microarray technique. Clone-to-clone variability of cells can be controlled in this inducible system. Taking this advantage, we investigated the response of the same cells to two different stimuli. We identified 20 genes (0.9% of 2304 transcripts examined) which showed twofold or more difference between with and without the core induction. Among them were several genes related to transcriptional regulation, signaling, RNA/protein metabolism, and apoptosis. We subsequently performed semiquantitative RT-PCR of four apoptosis-related genes and confirmed that ICAD and DAD1 were up-regulated, and TNFR1 and cytochrome c oxidase subunit VIII were down-regulated in the core-expressing cells.

With regard to ICAD, its promoter activity was up-regulated by the core protein expression and steady-state level of ICAD protein was subsequently increased. ICAD, otherwise known as DFF45 (DNA fragmentation factor 45-kDa subunit), is a caspase-3 substrate which is cleaved before apoptotic DNA fragmentation proceeds. Moreover, ICAD is a specific inhibitor of CAD, also called DFF40 (DNA fragmentation factor 40-kDa subunit), and is a molecular chaperone which is involved in proper folding of the endonuclease (reviewed by Nagata, 2000). It has been reported that overexpression of ICAD inhibits staurosporine- or Fas-induced DNA fragmentation (Sakahira et al., 1998). To our knowledge, the data presented here are the first to demonstrate increased expression of ICAD mediated by a viral protein through enhancing its promoter activity. In this study, we observed that in the core-expressing Hep191 cells expression of CAD did not change, as determined by Western blotting as well as cDNA microarray (data not shown). The maintenance of a 1:1 ratio of ICAD and CAD might be important for the homeostasis of normal cells, because an excess of ICAD will increase the threshold for downstream apoptotic signaling. Thus, our findings suggest that up-regulation of ICAD by HCV core protein may contribute to metabolic perturbation such as inhibition of apoptosis in HCV-infected hepatocytes.

The DAD1 gene, identified as a defender against apoptotic death gene, was also up-regulated. The DAD1 gene encodes a subunit of the oligosaccharyltransferase enzyme complex that initiates N-linked glycosylation (Nakashima et al., 1993). This protein plays a role in inhibition of apoptosis in some cultured cells (Yoshimi et al., 2000). Studies with mice carrying a null allele for DAD1 showed that this gene is required for proper processing of N-linked glycoproteins and for certain cell survival (Hong et al., 2000). It is also of interest that DAD1 gene is highly expressed in HCC cells compared to adjacent nontumorous liver tissues through differential display analysis (Tanaka et al., 2001).

TNFR1 is one of death receptors and relays death signals through a cytoplasmic sequence motif called the death domain. Upon TNF engagement, TNFR1 binds other death domain-containing proteins and subsequently leads to activation of caspases, resulting in apoptosis (for review, see Ashkenazi and Dixit, 1998). Down-regulation of TNFR1 in our study is not consistent with the previous report showing HCV core protein binds to the cytoplasmic domain of TNFR1 and enhances TNF-induced apoptosis of certain mouse and human cells. In these cells, the presence of core protein did not alter the expression of TNFR1 (Zhu et al., 1998, 2001). The difference in the conditions of either cell culture or core expression may be attributed to this discrepancy.

Cytochrome c oxidase is the terminal enzyme complex in the mitochondrial respiratory chain, and cytochrome c oxidase subunit VIII is one of the 13 subunits of the complex. A progressive reduction in respiratory activity of cytochrome c oxidase induces cytochrome c release in anti-Fas-triggered apoptotic cells (Hajek et al., 2001). The release from the mitochondrial intermembrane space into the cytosol involves the activation of the apoptotic protease cascade together with Apaf-1 and procaspase-9 (Li et al., 1997). Interestingly, cytochrome c release from mitochondria is inhibited in the liver of HCV protein-expressing transgenic mice, in which Fas-mediated apoptotic cell death was suppressed (Machida et al., 2001). Nevertheless, the underlying mechanism of cytochrome c release is not well known yet. Further studies on down-regulation of cytochrome c oxidase subunit VIII in relation to respiratory activity of cytochrome c oxidase and cytochrome c release in our experimental setting are necessary.

We characterized the effect of HCV core protein on the cytokine-mediated apoptotic pathway in Hep191 cells. The cytokines Fas ligand and TNF-α are the critical components necessary for triggering receptor-mediated cell death in vivo. We show here that the core protein confers resistance against apoptotic DNA fragmentation induced by either anti-Fas antibody or TNF-α (Figs. 5 and 6). Our data confirmed that the pleiotropic effects of PNA do not cause this phenomenon, since we found no influence on the Fas-mediated apoptosis in control HepRXR cells even with a high concentration of PNA (30 μM). To avoid clonal diversity during the selection of permanent transfectants, we also analyzed HepG2 cells transiently transfected with both core-expressing pIND191 and pVgRXR. We observed similar results of antiapoptotic response (data not shown).

Caspase-3 is recognized as an important effector molecule in the apoptotic pathway, and its activity arises following the cleavage of inactive proenzyme (procaspase-3) after Fas or TNFR is stimulated. We show here that expression of core protein inhibits caspase-3 activity induced by anti-Fas. It was shown by quantifying the enzyme activity in cell extracts and monitoring the level of inactive 32-kDa procaspase-3. Previously some reports indicated that HCV proteins, particularly core protein, are involved in augmentation of caspase activation induced by anti-Fas or TNF-α (Ruggieri et al., 1997; Hahn et al., 2000), whereas others indicated its suppression (Marusawa et al., 1999; Otsuka et al., 2002; Machida et al., 2001). Since different experimental systems were used in these studies, the observed inconsistency may be due to the possible involvement of cellular

factor(s) in certain cells. Alternatively, the expression level of the core protein may be different. A previous report from our laboratory demonstrated that the core protein sensitizes Fas-mediated apoptosis possibly accompanied by up-regulation of caspase-3 (Ruggieri et al., 1997). We used Hep39 cells in that study. Hep39 cells are also originated from HepG2 cells and constitutively expresses the HCV core protein. Subsequently, we compared the steady-state level of the core protein in Hep39 and in Hep191 cells established in this study. The level in Hep39 cells is 100- to 500-fold higher than in Hep191 cells treated with 10 μM PNA determined by FEIA (data not shown).

It is generally accepted that caspase-3 is the primary inactivator of ICAD and is mainly involved in proteolytic pathways that induce apoptotic internucleosomal DNA fragmentation (Wolf et al., 1999). The results in the present study suggest that up-regulation of ICAD and inhibition of caspase-3 activity induced by the core protein collaboratively play roles in blocking DNase activity of CAD and consequently in inhibiting DNA fragmentation in human liver cells, which express the viral protein at moderate levels comparable to that found in patients with chronic liver diseases.

In conclusion, we established a tightly regulated inducible expression system of HCV core protein in human liver cells, where expression of the viral protein is promptly induced to physiological levels. Transcriptional profiling, coupled with studies to confirm gene expression, in this system allowed us to identify several interesting genes that may be involved in cell growth or apoptosis. Evidence that the core protein modulates ICAD expression and the pathway of caspase-3 activation should contribute to the understanding of the molecular mechanisms of HCV persistence and chronic liver diseases. Functional studies in the future to evaluate the significance of potential core-regulated genes implicating not only in apoptosis but in other cellular processes may also provide new directions for the detailed investigation of HCV pathogenesis.

Materials and methods

Construction of inducible expression vector for HCV core protein

HCV cDNA (nt 342 to 914), coding for the entire core protein (aa 1 to 191), was excised from the *Bgl*II site of the pCAGC191 (Suzuki et al., 2001) and inserted, using standard cloning procedures (Sambrook et al., 1989), into the *Bam*HI site of the inducible expression vector pIND/Hygro (Invitrogen, Carlsbad, CA) to yield plasmid pIND191. This vector contains five ecdysone/glucocorticoid response elements which allow binding of the modified VgEcR for activation of gene transcription and inducible expression of HCV core protein gene under control of a Drosophila minimal heat shock promoter. Hygromycin resistance gene in the vector allows selection of stable transfectant in mammalian cells.

Establishment of an inducible cell line

Stock cultures of human hepatoblastoma HepG2 cells were maintained in Dulbecco's modified Eagle's medium (DMEM) supplemented with 10% FBS, 100 units/ml of penicillin, and 100 mg/ml of streptomycin and kept at 37°C in a 5% CO_2 incubator. To generate a stable cell line allowing tightly regulated expression of HCV core protein, HepG2 cells were cotransfected with both plasmid pIND191 and pVgRXR (Invitrogen). The latter vector that contains the gene conferring Zeocin resistance also encodes modified ecdysone receptor (VgEcR) and the retinoid X receptor. This vector thus provides an ecdysone functional heterodimeric receptor for activation of gene expression upon binding to an ecdysone analog, such as PNA (Invitrogen) (No et al., 1996).

Monolayers of HepG2 cells were transfected with the plasmids in the presence of Trans-IT LT1 (Mirus Corp. WI) according to the manufacturer's instructions. After transfection, transformants were selected in DMEM containing 500 μg/ml of Hygromycin (Roche Diagnostics, Basel, Switzerland) and 400 μg/ml of Zeocin (Invitrogen) for 3 to 5 weeks. Individual colonies were isolated and amplified, followed by screening inducible expression of HCV core protein. After 24 h of incubating the amplified clones in the medium with PNA at 10 μM, expression of the core protein was determined by a sensitive FEIA (Kashiwakuma et al., 1996) (see below). Stable cell lines, which allow tightly regulated expression of the core protein, were designated as Hep191.

To obtain a control cell line not expressing HCV core protein, HepG2 cells were transfected with the plasmid pVgRXR. After transfection, transformants were selected in DMEM medium containing 400 μg/ml of Zeocin. The isolated resistant colonies were designated as HepRXR.

Quantitation of HCV core protein

Hep 191 cells were induced to express HCV core protein using PNA at various concentrations ranging from 0.3 to 30 μM for indicated periods. Expressed core protein was quantitated by FEIA method as reported previously (Kashiwakuma et al., 1996). Briefly, cells were homogenized in a solution containing 0.3% Triton X-100, 1.5% (3-cholamidopropyl dimethylammonio) propanesulfonic acid, and 15% sodium dodecyl sulfate (SDS). After incubating at 56°C for 30 min, the samples were centrifuged at 1000 rpm for 5 min, and the supernatants were subjected to FEIA. Total protein concentration of the lysates was determined using the Pierce Micro BCA protein Assay Reagent Kit according to the manufacturer's instructions (Pierce, Rockford, IL).

Western blot analysis

Cells were washed with phosphate-buffered saline (PBS) and lysed in SDS sample buffer. Cell lysates were separated by 15 or 12.5% SDS–polyacrylamide gel electrophoresis (SDS–PAGE) and electrotransferred to polyvinylidene difluoride membrane (Immobilion; Millipore Ltd., Bredford, MA). After blocking in nonfat milk solution (Block Ace, Yukijirushi Co., Sapporo, Japan), the membranes were probed with the monoclonal antibody against HCV core protein (B2, ANOGEN, Missisauga, Canada), as a primary antibody diluted 1:200 and incubated for 1 h at 37°C. After being washed, the membranes were incubated with horseradish peroxidase conjugated sheep anti-mouse or anti-rabbit immunoglobulins as secondary antibodies. Antigen-antibody complexes were visualized by enhanced chemiluminescence detection system (ECL; Amersham Biosciences, Piscataway, NJ) according to the manufacturer's protocol.

Immunofluorescence microscopy

For indirect immunofluorescence staining of HCV core protein, Hep191 cells were grown in a tissue chamber slide in the presence of 30 μM PNA for 48 h and fixed with 4% paraformaldehyde, followed by permeabilizing with 0.2% Triton X-100. After blocking in nonfat milk solution (Block Ace), cells were incubated for 1 h with the anticore monoclonal antibody. Following washing, cells were incubated for 1 h with Biotin-conjugated antibody to mouse immunoglobulin (Sigma-Aldrich, St. Louis, MO). To increase sensitivity and specificity of the antigen detection, ExtrAvidin conjugated with FITC (Sigma-Aldrich) was then added and incubated for 1 h, followed by examining with a fluorescent microscopy.

Cell growth property

To test cell growth of Hep191, 6×10^4 cells per well were seeded into six-well tissue culture plates. Cells were cultured in DMEM with FBS 10 or 1% and the medium with and without 10 μM PNA was changed daily. Cells from triplicate wells were harvested and viable cells were counted every other day for 10 days by trypan blue dye exclusion.

RT-PCR

Total RNAs were extracted from Hep191 and HepRXR cells using SV Total RNA Isolation System (Promega, Madison, WI) according to the manufacturers' protocols. Three micrograms of total RNAs was reverse transcribed by Superscript II (Invitrogen) using oligo(dT) primer. Amplification procedure using specific PCR primers was as follows: after 3 min at 96°C, the reaction of 96°C for 30 s, 55°C for 30 s, 72°C for 1 min was repeated for 20–30 cycles, and finally 10 min at 72°C for one cycle. A minimum amount of PCR cycle was carried out to stay within the linear amplification process for each gene. PCR products were electrophoresed on 2.0% agarose/ethidium bromide gels.

Microarray analysis

Preparation procedure of cDNA microarray was described previously (Yoshikawa et al., 2000; Otsuka et al., 2001). Total RNAs from Hep191 in the presence or absence of PNA at 10 μM for 36 h were isolated with ISOGEN Reagent (Nippon Gene, Tokyo, Japan). Poly(A)$^+$ RNAs were obtained with Oligotex-dT 30 mRNA purification kit (TaKaRa Bio. Inc., Kyoto, Japan), according to the manufacturer's instructions. Fluorescent nucleotide Cy3-dUTP or Cy5-dUTP was incorporated during reverse transcription of the poly(A)$^+$ RNA. The probes were purified and concentrated by passing through Centricon-30 microconcetrators (Millipore). The different fluorescence-labeled probes were mixed and applied onto a microarray slide. Hybridization was carried out at 65°C overnight under a humidified condition. The array was washed, centrifuged, and then scanned with a fluorescence laser confocal slide scanner (Scan Array 4000, GSI Lumonics, Tokyo, Japan). Images were analyzed and fluorescence intensities were measured by Quant Array (GSI Lumonics). Genes showing changes in expression by twofold or more in the average of two experiments, where labeling with the fluorescent dyes were switched during the synthesis, were considered as differentially expressed genes.

Anti-Fas and TNF-α-induced apoptotic response

Hep191 and HepRXR were cultured in the presence of 10 μM PNA for 36 h, followed by treating with anti-Fas antibody (CH-11; MBL, Nagoya, Japan) or recombinant human TNF-α (Sigma-Aldrich). Anti-Fas antibody and TNF-α were used at final concentrations of 100 and 10 ng/ml, respectively. The minimum concentration of cycloheximide (CHX) required for anti-Fas-induced apoptosis was previously determined as a final concentration of 500 ng/ml (Marusawa et al., 1999). After 14 or 48 h from the start of anti-Fas- or TNF-α treatment, respectively, apoptotic cell death was measured by Cell Death Detection ELISAPLUS (Roche Diagnostics) according to the manufacturer's instructions. This assay is based on the specific determination of mononucleosomes and oligonucleosomes in the cytoplasmic fraction of apoptosis-induced cells. Anti-Fas-induced apoptotic response in Hep191 was also evaluated using the TUNEL procedure using In Situ Cell Death Detection Kit, Fluorescein (Roche Diagnostics). Cells incubated in chamber slides were fixed with 4% paraformaldehyde in PBS, followed by permeabilization with 0.1% Triton X-100 in 0.1% sodium citrate. DNA strand breaks generated during apoptosis were fluorescein-labeled and

detected by fluorescence microscopy. Caspase-3 activity in the anti-Fas-treated Hep191 was evaluated by the CaspACETM Assay System (Promega), according to the manufacturer's instructions. Cytosolic proteins were incubated with the colorimetric substrate Ac-DEVD-pNA in the presence or absence of the caspase inhibitor Z-VAD-FMK. Released pNA, *p*-nitroaniline, from the substrate upon cleavage by caspase-3 activity was monitored by a photometer at 405 nm. Total protein concentration of the cell lysates was determined using the Pierce Micro BCA protein Assay Reagent Kit (Pierce).

Luciferase assay

Human embryonic kidney 293T cells in 24-mm-diameter dishes were transfected with 0.5 μg of HCV-core expressing plasmid pCAGC191 or control pCAGGS, 0.2 μg of a reporter plasmid containing ICAD promoter either pIPT-2, -3, or -4 (Kawane et al., 1999), and 0.01 μg of pRL-TK (Promega). After 24 h, cells were harvested, and luciferase activities were determined by the Dual-Luciferase Reporter Assay System (Promega) as described previously (Aoki et al., 1998). The measured firefly luciferase activities were normalized for transfection efficiency using the values of Renilla luciferase activity determined from the same cell extracts.

Acknowledgments

This work was supported in part by the Second-Term Comprehensive 10-Year Strategy for Cancer Control, and Research on Human Genome, Tissue Engineering and Food Biotechnology from the Ministry of Health and Welfare, and the program for Promotion of Fundamental Studies in Health Sciences of the Organization for Drug ADR Relief, R&D Promotion, and Product Review of Japan. The authors thank Dr. Shigekazu Nagata (Osaka University, Osaka, Japan) for providing ICAD promoter/luciferase reporter constructs. They also thank Yohko Baba for technical assistance, and Tomoko Mizoguchi for the preparation of the manuscript. R. Sacco is an STA fellow of Japan International Science and Technology Exchange Center.

References

Aoki, Y., Aizaki, H., Shimoike, T., Tani, H., Ishii, K., Saito, I., Matsuura, Y., Miyamura, T., 1998. A human liver cell line exhibits efficient translation of HCV RNAs produced by a recombinant adenovirus expressing T7 RNA polymerase. Virology 250, 140–150.

Ashkenazi, A., Dixit, V.M., 1998. Death receptors: signaling and modulation. Science 281, 1305–1308.

Choo, Q.-L., Kuo, G., Weiner, A.J., Overby, L.R., Bradley, D.W., Houghton, M., 1989. Isolation of a cDNA clone derived from a blood-borne non-A, non-B viral hepatitis genome. Science 244, 359–362.

Dubrez, L., Savoy, I., Hamman, A., Solary, E., 1996. Pivotal role of a DEVD- sensitive step in etoposide-induced and Fas-mediated apoptotic pathways. EMBO J. 15, 5504–5512.

Dumoulin, F.L., von dem Bussche, A., Sohne, J., Sauerbruch, T., Spengler, U., 1999. Hepatitis C virus core protein does not inhibit apoptosis in human hepatoma cells. Eur. J. Clin. Invest. 29, 940–946.

Enari, M., Sakahira, H., Yokoyama, H., Okawa, K., Iwamatsu, A., Nagata, S., 1998. A caspase-activated DNase that degrades DNA during apoptosis, and its inhibitor ICAD. Nature 391, 43–50.

Fujita, T., Ishido, S., Muramatsu, S., Itoh, M., Hotta, H., 1996. Suppression of actinomycin D-induced apoptosis by the NS3 protein of hepatitis C virus. Biochem. Biophys. Res. Commun. 229, 825–831.

Gale Jr., M., Kwieciszewski, B., Dossett, M., Nakao, H., Katze, M.G., 1999. Antiapoptotic and oncogenic potentials of hepatitis C virus are linked to interferon resis. PG. J. Virol. 73, 6506–6516.

Hahn, C.S., Cho, Y.G., Kang, B.S., Lester, I.M., Hahn, Y.S., 2000. The HCV core protein acts as a positive regulator of fas-mediated apoptosis in a human lymphoblastoid T cell line. Virology 276, 127–137.

Hajek, P., Villani, G., Attardi, G., 2001. Rate-limiting step preceding cytochrome c release in cells primed for Fas-mediated apoptosis revealed by analysis of cellular mosaicism of respiratory changes. J. Biol. Chem. 276, 606–615.

Hayashi, N., Mita, E., 1997. Fas system and apoptosis in viral hepatitis. J. Gastroenterol. Hepatol. 12, S223–226.

Honda, M., Kaneko, S., Shimazaki, T., Matsushita, E., Kobayashi, K., Ping, L.H., Zhang, H.C., Lemon, S.M., 2000. Hepatitis C virus core protein induces apoptosis and impairs cell-cycle regulation in stably transformed Chinese hamster ovary cells. Hepatology 31, 1351–1359.

Hong, N.A., Flannery, M., Hsieh, S.N., Cado, D., Pedersen, R., Winoto, A., 2000. Mice lacking Dad1, the defender against apoptotic death-1, express abnormal N-linked glycoproteins and undergo increased embryonic apotosis. Dev. Biol. 220, 76–84.

Kashiwakuma, T., Hasegawa, A., Kajita, T., Takata, A., Mori, H., Ohta, Y., Tanaka, E., Kiyosawa, K., Tanaka, T., Tanaka, S., Hattori, N., Kohara, M., 1996. Detection of hepatitis C virus specific core protein in serum of patients by a sensitive fluorescence enzyme immunoassay (FEIA). J. Immunol. Methods 190, 79–89.

Kawane, K., Fukuyama, H., Adachi, M., Sakahira, H., Copeland, N.G., Gilbert, D.J., Jenkin, N.A., Nagata, S., 1999. Structure and promoter analysis of murine CAD and ICAD genes. Cell Death Differ. 6, 745–752.

Koike, K., Tsutsumi, T., Fujie, H., Shintani, Y., Kyoji, M., 2002. Molecular mechanism of viral hepatocarcinogenesis. Oncology 62 (Suppl. 1), 29–37.

Kuo, G., Choo, Q.L., Alter, H.J., Gitnick, G.L., Redeker, A.G., Purcell, R.H., Miyamura, T., Dienstag, J.L., Alter, M.J., Stevens, C.E., et al., 1989. An assay for circulating antibodies to a major etiologic virus of human non-A, non-B hepatitis. Science 244, 362–364.

Lacronique, V., Mignon, A., Fabre, M., Viollet, B., Rouquet, N., Molina, T., Porteu, A., Henrion, A., Bouscary, D., Varlet, P., Joulin, V., Kahn, A., 1996. Bcl-2 protects from lethal hepatic apoptosis induced by an anti-Fas antibody in mice. Nat. Med. 2, 80–86.

Lai, M.M.C., Ware, C.F., 1999. Hepatitis C virus core protein: possible roles in viral pathogenesis, in: Hagedorn, C.H., Rice, C.M. (Eds.), The Hepatitis C Viruses, Springer, Berlin, pp. 117–134.

Lau, J.Y., Xie, X., Lai, M.M., Wu, P.C., 1998. Apoptosis and viral hepatitis. Semin. Liver Dis. 18, 169–176.

Li, K., Prow, T., Lemon, S.M., Beard, M.R., 2002. Cellular response to conditional expression of hepatitis C virus core protein in Huh7 cultured human hepatoma cells. Hepatology 35, 1237–1246.

Li, P., Nijhawan, D., Budihardjo, I., Srinivasula, S.M., Ahmad, M., Alnemri, E.S., Wang, X., 1997. Cytochrome c and dATP-dependent formation of Apaf- 1/caspase-9 complex initiates an apoptotic protease cascade. Cell 91, 479–489.

Liu, X., Zou, H., Slaughter, C., Wang, X., 1997. DFF, a heterodimeric protein that functions downstream of caspase-3 to trigger DNA fragmentation during apoptosis. Cell 89, 175–184.

Machida, K., Tsukiyama-Kohara, K., Seike, E., Tone, S., Shibasaki, F., Shimizu, M., Takahashi, H., Hayashi, Y., Funata, N., Taya, C., Yonekawa, H., Kohara, M., 2001. Inhibition of cytochrome c release in Fas-mediated signaling pathway in transgenic mice induced to express hepatitis C viral proteins. J. Biol. Chem. 276, 12140–12146.

Marusawa, H., Hijikata, M., Chiba, T., Shimotohno, K., 1999. Hepatitis C virus core protein inhibits Fas- and tumor necrosis factor alpha-mediated apoptosis via NF-kappaB activation. J. Virol. 73, 4713–4720.

Moradpour, D., Englert, C., Wakita, T., Wands, J.R., 1996. Characterization of cell lines allowing tightly regulated expression of hepatitis C virus core protein. Virology 222, 51–63.

Nagata, S., 2000. Apoptotic DNA fragmentation. Exp. Cell Res. 256, 12–18.

Nakashima, T., Sekiguchi, T., Kuraoka, A., Fukushima, K., Shibata, Y., Komiyama, S., Nishimoto, T., 1993. Molecular cloning of a human cDNA encoding a novel protein, DAD1, whose defect causes apoptotic cell death in hamster BHK21 cells. Mol. Cell. Biol. 13, 6367–6374.

No, D., Yao, T.P., Evans, R.M., 1996. Ecdysone-inducible gene expression in mammalian cells and transgenic mice. Proc. Natl. Acad. Sci. USA 93, 3346–3351.

Ogasawara, J., Watanabe-Fukunaga, R., Adachi, M., Matsuzawa, A., Kasugai, T., Kitamura, Y., Itoh, N., Suda, T., Nagata, S., 1993. Lethal effect of the anti- Fas antibody in mice. Nature 364, 806–809.

Otsuka, M., Kato, N., Taniguchi, H., Yoshida, H., Goto, T., Shiratori, Y., Omata, M., 2002. Hepatitis C virus core protein inhibits apoptosis via enhanced Bcl-xL expression. Virology 296, 84–93.

Otsuka, M., Kato, M., Yoshikawa, T., Chen, H., Brown, E.J., Masuho, Y., Omata, M., Seki, N., 2001. Differential expression of the L-plastin gene in human colorectal cancer progression and metastasis. Biochem. Biophys. Res. Commun. 289, 876–881.

Patel, T., Roberts, L.R., Jones, B.A., Gores, G.J., 1998. Dysregulation of apoptosis as a mechanism of liver disease: an overview. Semin. Liver Dis. 18, 105–114.

Ray, R.B., Meyer, K., Ray, R., 1996. Suppression of apoptotic cell death by hepatitis C virus core protein. Virology 226, 176–182.

Ray, R.B., Meyer, K., Steele, R., Shrivastava, A., Aggarwal, B.B., Ray, R., 1998. Inhibition of tumor necrosis factor (TNF-alpha)-mediated apoptosis by hepatitis C virus core protein. J. Biol. Chem. 273, 2256–2259.

Ruggieri, A., Harada, T., Matsuura, Y., Miyamura, T., 1997. Sensitization to Fas- mediated apoptosis by hepatitis C virus core protein. Virology 229, 68–76.

Saito, I., Miyamura, T., Ohbayashi, A., Harada, H., Katayama, T., Kikuchi, S., Watanabe, Y., Koi, S., Onji, M., Ohta, Y., Choo, Q.-L., Houghton, M., Kuo, G., 1990. Hepatitis C virus infection is associated with the development of hepatocellular carcinoma. Proc. Natl. Acad. Sci. USA 87, 6547–6549.

Sakahira, H., Enari, M., Nagata, S., 1998. Cleavage of CAD inhibitor in CAD activation and DNA degradation during apoptosis. Nature 391, 96–99.

Sambrook, J., Fritsch, E.F., Maniatis, T., 1989. Molecular Cloning: A Laboratory Manual. Cold Spring Harbor Laboratory Press, Cold Spring Harbor, NY.

Suzuki, R., Suzuki, T., Ishii, K., Matsuura, Y., Miyamura, T., 1999. Processing and functions of Hepatitis C virus proteins. Intervirology 42, 145–152.

Suzuki, R., Tamura, K., Li, J., Ishii, K., Matsuura, Y., Miyamura, T., Suzuki, T., 2001. Ubiquitin-mediated degradation of hepatitis C virus core protein is regulated by processing at its carboxyl terminus. Virology 280, 301–309.

Tai, D.I., Tsai, S.L., Chen, Y.M., Chuang, Y.L., Peng, C.Y., Sheen, I.S., Yeh, C.T., Chang, K.S., Huang, S.N., Kuo, G.C., Liaw, Y.F., 2000. Activation of nuclear factor kappaB in hepatitis C virus infection: Implications for pathogenesis and hepatocarcinogenesis. Hepatology 31, 656–664.

Tanaka, K., Kondoh, N., Shuda, M., Matsubara, O., Imazeki, N., Ryo, A., Wakatsuki, T., Hada, A., Goseki, N., Igari, T., Hatsuse, K., Aihara, T., Horiuchi, S., Yamamoto, N., Yamamoto, M., 2001. Enhanced expression of mRNAs of antisecretory factor-1, gp96, DAD1 and CDC34 in human hepatocellular carcinomas. Biochem. Biophys. Acta 1536, 1–12.

Thomson, M., Liang, T.J., 2000. Molecular biology of hepatitis C virus. in: Liang, T.J., Hoofnagle, J.H. (Eds.). Hepatitis C. Academic Press, San Diegopp, pp. 1–24.

Tsutsumi, T., Suzuki, T., Moriya, K., Yotsuyanagi, H., Shintani, Y., Fujie, H., Matsuura, Y., Kimura, S., Koike, K., Miyamura, T., 2003. Alteration of intrahepatic cytokine expression and AP-1 activation in transgenic mice expressing hepatitis C virus core protein. Virology 00, 000–000.

Wolf, B.B., Schuler, M., Echeverri, F., Green, D.R., 1999. Caspase-3 is the primary activator of apoptotic DNA fragmentation via DNA fragmentation factor- 45/inhibitor of caspase-activated DNase inactivation. J. Biol. Chem. 274, 30651–30656.

Yoshikawa, T., Nagasugi, Y., Azuma, T., Kato, M., Sugano, S., Hashimoto, K., Masuho, Y., Muramatsu, M., Seki, N., 2000. Isolation of novel mouse genes differentially expressed in brain using cDNA microarray. Biochem. Biophys. Res. Commun. 275, 532–537.

Yoshimi, M., Sekiguchi, T., Hara, N., Nishimoto, T., 2000. Inhibition of N-linked glycosylation causes apoptosis in hamster BHK21 cells. Biochem. Biophys. Res. Commun. 276, 965–969.

Zhu, N., Khoshnan, A., Schneider, R., Matsumoto, M., Dennert, G., Ware, C., Lai, M.M., 1998. Hepatitis C virus core protein binds to the cytoplasmic domain of tumor necrosis factor (TNF) receptor 1 and enhances TNF-induced apoptosis. J. Virol. 72, 3691–3697.

Zhu, N., Ware, C.F., Lai, M.M., 2001. Hepatitis C virus core protein enhances FADD-mediated apoptosis and suppresses TRADD signaling of tumor necrosis factor receptor. Virology 283, 178–187.

JOURNAL OF VIROLOGY, Dec. 2003, p. 13335–13347 Vol. 77, No. 24
0022-538X/03/$08.00+0 DOI: 10.1128/JVI.77.24.13335–13347.2003

Complete Genomic Sequence and Comparative Analysis of the Tumorigenic Poxvirus Yaba Monkey Tumor Virus

Craig R. Brunetti,[1]† Hiroko Amano,[2] Yoshiaki Ueda,[2] Jing Qin,[1] Tatsuo Miyamura,[2] Tetsuro Suzuki,[2] Xing Li,[3] John W. Barrett,[1] and Grant McFadden[1,4]*

BioTherapeutics Research Group, Robarts Research Institute, London, Ontario, Canada N6G 2V4[1]; Department of Microbiology and Immunology, University of Western Ontario, London, Ontario, Canada N6A 5C1[4]; Laboratory of Tumor Viruses, National Institute of Infectious Diseases, Tokyo 162-8640, Japan[2]; and Viron Therapeutics Inc., London, Ontario, Canada N5G 2V4[3]

Received 15 July 2003/Accepted 4 September 2003

The *Yatapoxvirus* genus of poxviruses is comprised of *Yaba monkey tumor virus* (YMTV), *Tanapox virus*, and *Yaba-like disease virus* (YLDV), which all have the ability to infect primates, including humans. Unlike other poxviruses, YMTV induces formation of focalized histiocytomas upon infection. To gain a greater understanding of the *Yatapoxvirus* genus and the unique tumor formation properties of YMTV, we sequenced the 134,721-bp genome of YMTV. The genome of YMTV encodes at least 140 open reading frames, all of which are also found as orthologs in the closely related YLDV. However, 13 open reading frames found in YLDV are completely absent from YMTV. Common to both YLDV and YMTV are the unusually large noncoding regions between many open reading frames. To determine whether any of these noncoding regions might be functionally significant, we carried out a comparative analysis between the putative noncoding regions of YMTV and similar noncoding regions from other poxviruses. This approach identified three new gene poxvirus families, defined as orthologs of YMTV23.5L, YMTV28.5L, and YMTV120.5L, which are highly conserved in virtually all poxvirus species. Furthermore, the comparative analysis also revealed a 40-bp nucleotide sequence at approximately 14,700 bases from the left terminus that was 100% identical in the comparable intergene site within members of the *Yatapoxvirus*, *Suipoxvirus*, and *Capripoxvirus* genera and 95% conserved in the *Leporipoxvirus* genus. This conserved sequence was shown to function as a poxvirus late promoter element in transfected and infected cells, but other functions, such as an involvement in viral replication or packaging, cannot be excluded. Finally, we summarize the predicted immunomodulatory protein repertoire in the *Yatapoxvirus* genus as a whole.

Poxviruses are divided into two major groups, the chordopoxviruses that infect vertebrates and entomopoxviruses of insects. Chordopoxviruses contain a linear double-stranded DNA genome with covalently closed hairpin loops at either end (19). The extreme left and right termini of the poxvirus genome consist of identical, but oppositely oriented, terminal inverted repeats (TIR). Chordopoxvirus genomes can be divided into two broad domains based on the functions of the encoded gene products. The central region of the genome, which ranges in length from 80,000 to 100,000 bases, is enriched for genes that encode essential conserved functions, such as transcription, replication, and virion assembly. The regions flanking this conserved central region express an array of proteins that function to increase survival of the virus in the infected host, including proteins that determine host range, inhibit apoptosis, or mediate responses to modulate the host immune system (22).

The genome sizes of published chordopoxviruses vary from 145,000 bp for Yaba-like disease virus (YLDV) (15) up to 288,000 bp for fowlpox virus (2) and possess between 151 and 260 assigned open reading frames (ORFs). Complete genomic sequences of representative members from seven of the eight *Chordopoxvirus* genera have now been published, including orthopoxviruses (vaccinia virus strain Copenhagen [11], modified vaccinia virus strain Ankara [6], variola virus strain Bangladesh [16], variola virus strain India [24], variola virus strain Garcia [25], camelpox virus [1], and monkeypox virus [26]), capripoxviruses (lumpy skin disease virus [LSDV] [29], goatpox virus, and sheeppox virus [30]), leporipoxviruses (myxoma virus [8] and Shope fibroma virus [31]), suipoxviruses (swinepox virus [SPV] [3]), molluscipoxvirus (molluscum contagiosum virus [23]), avipoxviruses (fowlpox [2]), and yatapoxviruses (Yaba-like disease virus [YLDV] [15]).

The *Yatapoxvirus* genus of poxviruses is comprised of three virus isolates: YLDV, *Tanapox virus* (TPV), and *Yaba monkey tumor virus* (YMTV) (14). The yatapoxviruses have a narrow host range, infecting only primates, including humans. Several pieces of data suggest that TPV and YLDV may be different strains of the same virus. For example, TPV and YLDV produce a clinically indistinguishable disease, which includes a mild fever and epidermal lesions (10, 17), and the published genomic sequence of YLDV is more than 98.6% identical with the 8,300 bases of TPV sequence entered into the public database (GenBank accession no. AY253325, AF245394, and AF153912) (15). This level of sequence identity is comparable to different strains of vaccinia virus and suggests that YLDV and TPV should be considered the monkey and human versions, respectively, of the same virus.

* Corresponding author. Mailing address: BioTherapeutics Research Group, Robarts Research Institute, 1400 Western Rd., London, Ontario, Canada N6G 2V4. Phone: (519) 663-3184. Fax: (519) 663-3847. E-mail: mcfadden@robarts.ca.

† Present address: Department of Biology, Trent University, Peterborough, Ontario K9L 7B8, Canada.

YMTV was originally characterized to be the agent responsible for subcutaneous tumors in a rhesus monkey colony occurring in 1956 in Yaba, Nigeria (7). YMTV is one of the few poxviruses that induce substantial tumor formation upon infection (5, 12, 20, 27). In rhesus monkeys infected with YMTV, the tumors are thought to be derived from histiocytes that migrate to the site of infection. The histiocytes become infected and begin to rapidly proliferate, become multinucleated, and eventually form a polyclonal tumor (27). However, the tumors generally do not become invasive and spontaneously regress, presumably when either viral cytopathic effect kills the infected cells or cell-mediated antiviral immunity becomes sufficiently effective to clear the infection (12, 27).

The complete genomic sequence of YLDV was recently published, and a number of novel ORFs not found in other chordopoxviruses were identified (15). As well, despite the fact that the noncoding regions between ORFs in most poxviruses are typically only a few nucleotides, there were multiple identified inter-ORF regions of 200 or more nucleotides in YLDV. Typically, the minimum size for a poxvirus ORF is arbitrarily set (e.g., 30 amino acids for SPV, LSDV, molluscum contagiosum virus, and fowlpox virus [2, 3, 23, 29]; 50 amino acids for myxoma virus [8]; and 60 amino acids for YLDV [15]). If bona fide ORFs were indeed located within these assigned YLDV noncoding regions, then one would predict that these ORFs might be highly conserved between YLDV and YMTV. Therefore, in an effort to understand the clinical differences between YLDV and YMTV and to provide a closely related sequence to YLDV for a comparative genomic approach, we sequenced the genome of the YMTV and provide a comparative genomic analysis of the *Yatapoxvirus* genus.

MATERIALS AND METHODS

Viruses. YMTV (VR587) was obtained from the American Type Culture Collection (Manassas, Va.) and was propagated on CV1 cells at 35°C in minimum essential medium containing 5% fetal bovine serum. Myxoma virus strain Lausanne was obtained from the American Type Culture Collection and propagated in BGMK cells at 37°C.

Isolation and sequencing of YMTV genomic fragments. YMTV genomic DNA was isolated from infected CV1 cells and was subjected to restriction enzyme digestion with *Pst*I, *Bam*HI, *Sal*I, *Xba*I, or *Eco*RI. The digested DNA was cloned into pUC19 or pBR322 vectors and sequenced by the dideoxy sequencing method (21). The remainder of the YMTV genomic sequence was cloned using overlapping PCR. Briefly, PCR was carried out using *Taq* polymerase, YMTV genomic DNA, and PCR primers based on the corresponding sequence of YLDV (15). The resulting PCR products were cloned into pGEMT-easy (Promega, Madison, Wis.) and were sequenced by the London Regional Genomics Centre DNA Sequencing Facility using an Applied Biosystems (Foster City, Calif.) ABI Prism 377 DNA sequencer and Big Dye terminators (Applied Biosystems). Some of the YMTV sequence was previously submitted to GenBank (accession no. AY253324, AB025319, AB018404, and AB015885).

Sequence analysis. The sequence data were assembled using Sequencher 3.0, and ORFs were identified using MacVector 6.5.3 (Oxford Molecular Ltd.).

Cloning a conserved sequence from myxoma virus upstream of an enhanced GFP cassette. PCR was carried out using *Taq* polymerase; plasmid DNA pEGFP-N1 (Clontech, Palo Alto, Calif.); the reverse PCR primer 5′ TTACGC CTTAAGATACATTG 3′, which corresponds to the 3′ end of the green fluorescent protein (GFP), and the forward PCR primers (with the start codon of GFP in boldface type) 5′ TCGCCACCATGGTGAGCAAG 3′ (PCR-GFP), 5′ TTTATTTATGTTATTAGCTAGGATTTATGTTTCATTTTTTACTCGCCA CCATGGTGAGCAAG 3′ (PCR-R-GFP), and 5′ GTAAAAAATGAAACATA AATCCTAGCTAATAACATAAATAAATCGCCACCATGGTGAGCAAG 3′ (PCR-L-GFP). The resulting PCR products were cloned into pGEMT-easy (Promega) and designated GFP, R-GFP, and L-GFP.

Expression of GFP cassette in BGMK cells. Twelve-well dishes of BGMK cells approximately 90% confluent growing in minimum essential medium–5% fetal bovine serum were either infected with myxoma virus at a multiplicity of infection of 10 or mock infected. The cells were incubated at 37°C for 2 h, and this was followed by transfection with GFP, R-GFP, or L-GFP plasmid DNA using Lipofectamine Plus (Invitrogen, Burlington, Ontario, Canada) per the manufacturer's protocol. The cells were subsequently incubated at 37°C for 48 h. Cells expressing the GFP construct were detected using a fluorescence microscope.

Nucleotide sequence accession number. Sequence data from this article have been deposited in GenBank under accession number AY386371.

RESULTS

Genome structure of YMTV. The genome of YMTV was sequenced through the subcloning of genomic fragments into plasmid vectors, and clones were individually sequenced. In addition, regions of the genome not represented in the cloned fragments were isolated using PCR, and a minimum of three independent PCR products for each primer set were sequenced. After assembling the sequence files, a single continuous sequence of 134,721 bases was generated, making YMTV the smallest poxvirus genome yet sequenced. This deduced sequence lacks the terminal hairpin region, but evidence suggests that all the coding ORFs have been fully sequenced and only the very extreme hairpin termini of the genome were not included. In particular, the putative YMTV concatemer resolution sequence was obtained, which is typically found very close to the molecular hairpin loop at the termini (18). Published reports also confirm that the YMTV genome size is indeed approximately 135,000 bases (4).

The YMTV genome has an A+T content of 70.2% and encodes at least 140 ORFs (Table 1; Fig. 1), of which 139 are single copies and 1 is repeated in each copy of the TIR. In comparison, YLDV has been assigned 151 ORFs (15). YMTV and YLDV is closely related viruses with approximately 75% identity between the viruses at the nucleotide level overall, which is typical for chordopoxvirus members from a single genus. Furthermore, all the ORFs identified in YMTV have a corresponding ortholog in YLDV, but YMTV has lost 13 ORFs that are present in YLDV (Table 2), which accounts for the 10 kb of sequence loss in YMTV. Since YMTV and YLDV are so similar, and to avoid unnecessary confusion, we have adopted the proposed YLDV nomenclature (15) for naming orthologous YMTV ORFs.

The TIR of YMTV are 1,962 bases long and contain a single ORF designated 1L/151R. The noncoding region in the TIR of YMTV and YLDV is relatively large, with 804 and 755 bases (15), respectively, between the terminal ORF and the concatemer resolution sequence. In comparison, closely related genera, such as members of the *Capripoxvirus*, *Leporipoxvirus*, and *Suipoxvirus* genera, have noncoding regions in their termini ranging from 159 to 366 bases (3, 8, 29). Analysis of the noncoding region from YMTV and YLDV revealed a nucleotide sequence in each that exhibited striking similarity to that of the SPV002 gene (Fig. 2). However, both the YMTV and YLDV sequences lack an initiating methionine (ATG) codon, suggesting that either the large noncoding sequence in the TIR of yatapox viruses has evolved into a pseudogene of SPV002, or else the yatapox virus orthologs utilize a nonstandard initiator codon.

Identification of putative orthologs of YMTV23.5L in mul-

TABLE 1. YMTV ORFs

ORF	Codon		No. of aa	TOL[a]	Predicted structure or function[b]	YLDV[a]			SPV[b]		Myx[c]		LSDV[d]		VV[e]	
	Start	Stop				ORF	BLASTP2 score	% Identity	ORF	% Identity	ORF	% Identity	ORF	% Identity	ORF	% Identity
1L	1808	804	334	E	A52R family	1L	489	72					LSDV007	35	C10L	26
2L	2963	1938	341	?	vTNF-α bp, SP	2L	497	71	SPV003	34						
4L	3722	3003	239	?	α-Amanitin sensitivity	4L	340	71	SPV007	28			LSDV009	35	N2L	31
5L	4232	3762	156	L	LAP/PHD finger, TM	5L	200	58	SPV009	36	M153R	32	LSDV010	48		
6L	4732	4274	152	E	Unknown	6L	265	81	SPV001/150	37	M003.1	28	LSDV001/156	34	B15R	41
7L	5840	4800	346	E?	vCCR8	7L	265	70	SPV005				LSDV011	39		
11L	8306	6393	637	?	14 ankyrin domains	11L	1061	79								
12L	8574	8308	88	E	eIF2α mimic	12L	111	64	SPV010	36	M156R	32	LSDV014	35	K3L	31
13L	9474	8614	286	L	Monoglyceride lipase	13L	406	68							K6L	48
14L	9917	9504	137	I?	IL-18 bp, SP	14L	156	55	SPV011	30			LSDV015	37		
16L	10584	10066	172	L?	Inhibition of apoptosis	16L	207	64	SPV012	29			LSDV017	30	I1L	24
17L	11066	10635	143	L?	dUTPase	17L	215	75	SPV013	52	M012L	48	LSDV018	52	F2L	46
19L	12774	11200	524	L?	Kelch-like protein	19L	820	74	SPV015	35	M014L	32	LSDV019	34	F3L	25
20L	13779	12802	325	L	Ribonucleotide reductase (small subunit)	20L	611	91	SPV016	76	M015L	75	LSDV020	79	F4L	76
21L	14054	13806	82	?	SP, TM	21L	114	64	SPV017	33	M016L	42	LSDV021	31		
22L	14325	14098	75	E	Unknown	22L	45	37								
23.5L	14742	14530	70	E	Unknown	23.5L	88	86			M018L	45	LSDV023	57	F8L	43
24L	15443	14799	214	L	TM	24L	312	74	SPV021	45	M019L	43	LSDV024	43	F9L	48
25L	16758	15421	445	L	Ser/Thr protein kinase	25L	845	90	SPV022	77	M020L	74	LSDV025	77	F10L	72
26L	18711	16786	642	L	TM	26L	861	65	SPV024	42	M021L	37	LSDV027	40	F12L	31
27L	19845	18736	369	L	EEV envelope protein	27L	657	87	SPV025	70	M022L	69	LSDV028	72	F13L	57
28.5L	20085	19909	58	L	Unknown	28.5L										
29L	20563	20117	148	?	Unknown	29L	263	82	SPV027	60	M024L	49	LSDV029	62	F15L	56
30L	21275	20628	215	?	Unknown	30L	320	73	SPV028	38	M025L	30	LSDV030	36	F16L	37
31R	21335	21649	104	L	DNA binding phosphoprotein	31R	169	79	SPV029	62	M026L	68	LSDV031	63	F17R	59
32L	23058	21646	470	?	Poly(A) polymerase	32L	832	88	SPV030	67	M027L	68	LSDV032	68	E1L	64
33L	25120	23072	683	?	Unknown	33L	1006	71	SPV031	44	M028L	40	LSDV033	40	E2L	37
34L	25700	25146	185	L	dsRNA bp	34L	217	57	SPV032	44	M029L	57	LSDV034	42	E3L	38
35L	26311	25745	188	L	RNA polymerase subunit RPO30	35L	326	82	SPV033	66	M030L	64	LSDV036	63	E4L	67
36R	26444	27472	342	L?	Unknown	36R	512	71			M031R	31	LSDV035	33	E5R	25
37R	27498	29201	567	L?	Unknown	37R	1006	85	SPV034	65	M032R	61	LSDV037	67	E6R	60
38R	29219	30025	268	L	ER-localized protein, TM	38R	521	93	SPV035	76	M033R	75	LSDV038	78	E8R	70
39L	33042	30022	1006	?	DNA polymerase	39L	1689	81	SPV036	64	M034L	66	LSDV039	66	E9L	63
40R	33075	33359	94	L	Redox protein	40R	181	88	SPV037	67	M035R	69	LSDV040	71	E10R	67
41L	33770	33393	125	L	TM	41L	200	74					LSDV041	53	E11L	48
43L	34881	33955	308	L	DNA binding protein	43L	472	77	SPV039	60	M038L	64	LSDV043	66	I1L	60
44L	35103	34882	73	L	TM	44L	116	77	SPV040	48	M039L	52	LSDV044	51	I2L	45
45L	35898	35104	264	E?	DNA binding phosphoprotein	45L	437	84	SPV041	60	M040L	61	LSDV045	58	I3L	56
46L	36227	35988	79	L	IMV protein, SP, TM	46L	138	86	SPV043	55	M041L	48	LSDV046	69	I5L	45
47L	37402	36245	385	L	TM	47L	625	79	SPV044	51	M042L	52	LSDV047	53	I6L	54
48L	38688	37399	429	L	Virion core protein	48L	773	87	SPV045	69	M043L	69	LSDV048	71	I7L	64
49R	38694	40730	678	?	NPH-II, RNA helicase	49R	1133	80	SPV046	58	M044R	54	LSDV049	59	I8R	54
50L	42496	40727	590	L	Metalloproteinase	50L	963	78	SPV047	59	M045L	55	LSDV050	57	G1L	51
51L	42828	42493	111	L	TM	51L	167	71	SPV049	54	M046L	48	LSDV052	47	G3L	41
52R	42822	43490	222	?	Transcriptional elongation factor	52R	349	78	SPV048	45	M047R	44	LSDV051	46	G2R	47
53L	43834	43457	125	L	Glutaredoxin 2	53L	255	99	SPV050	64	M048L	69	LSDV053	75	G4L	45
54R	43837	45156	439	?	Unknown	54R	672	76	SPV051	49	M049R	44	LSDV054	49	G5R	43
55R	45159	45350	63	?	RNA polymerase subunit, RPO7	55R	125	96	SPV052	84	M050R	85	LSDV055	85	G5.5R	79
56R	45350	45895	181	L	TM	56R	291	79	SPV053	53	M051R	57	LSDV056	54	G6R	47
57L	46964	45864	366	L	Virion core protein, TM	57L	580	78	SPV054	53	M052L	52	LSDV057	55	G7L	48
58R	46994	47776	260	L	Late transcription factor, VLTF-1, TM	58R	511	97	SPV055	88	M053R	83	LSDV058	86	G8R	83
59R	47808	48806	332	L	Myristylated protein	59R	528	78	SPV056	52	M054R	53	LSDV059	57	G9R	45
60R	48807	49550	247	L	Myristylated IMV envelope protein	60R	452	91	SPV057	82	M055R	75	LSDV060	80	L1R	69
61R	49565	49840	91	?	TM	61R	99	57	SPV058	32			LSDV061	34		
62L	50763	49816	315	L	Unknown	62L	518	80	SPV059	59	M057L	54	LSDV062	60	L3L	51
63R	50788	51546	252	L	DNA binding protein	63R	455	92	SPV060	76	M058R	77	LSDV063	79	L4R	60
64R	51566	51964	132	L	TM	64R	181	68	SPV061	46	M059R	44	LSDV064	50	L5R	44

Continued on following page

TABLE 1—*Continued*

ORF	Codon		No. of aa[f]	TOL[g]	Predicted structure or function[h]	YLDV[a]			SPV[b]		Myx[c]		LSDV[d]		VV[e]	
	Start	Stop				ORF	BLASTP2 score	% Identity	ORF	% Identity	ORF	% Identity	ORF	% Identity	ORF	% Identity
65R	51906	52385	159	L	Unknown	65R	275	83	SPV062	58	M060R	58	LSDV065	65	J1R	47
66R	52382	52927	181	E?	Thymidine kinase	66R	287	78	SPV063	62	M061R	61	LSDV066	58	J2R	61
67R	52968	53471	167	L	Host range protein	67R	283	81	SPV064	45	M062R	38	LSDV067	44	C7L	37
68R	53549	54550	333	?	Poly(A) polymerase	68R	583	85	SPV065	69	M065R	70	LSDV068	72	J3R	67
69R	54465	55022	185	?	RNA polymerase subunit, RPO22	69R	317	91	SPV066	75	M066R	72	LSDV069	78	J4R	72
70L	55412	54999	137	L	Unknown	70L	251	82	SPV067	62	M067L	62	LSDV070	64	J5L	60
71R	55509	59366	1285	L	RNA polymerase subunit, RPO147	71R	2382	91	SPV068	81	M068R	82	LSDV071	82	J6R	78
72L	59872	59363	169	L	Protein tyrosine phosphatase	72L	317	88	SPV069	71	M069L	74	LSDV072	77	H1L	63
73R	59887	60456	189	L?	TM	73R	340	84	SPV070	67	M070R	65	LSDV073	67	H2R	61
74L	61420	60458	320	L	IMV envelope protein, TM	74L	498	79	SPV071	55	M071L	50	LSDV074	53	H3L	36
75L	63814	61421	797	L	RNA polymerase-associated protein, RAP94	75L	1388	86	SPV072	71	M072L	70	LSDV075	72	H4L	64
76R	64007	64549	180	L?	Late transcription factor VLTF-4	76R	205	61	SPV073	41	M073R	40	LSDV076	34	H5R	34
77R	64560	65507	315	?	DNA topoisomerase	77R	536	83	SPV074	62	M074R	64	LSDV077	68	H6R	63
78R	65515	65967	150	L	Unknown	78R	246	80	SPV075	54	M075R	53	LSDV078	50	H7R	36
79R	65982	68504	840	L	mRNA capping enzyme (large subunit)	79R	1462	85	SPV076	65	M076R	65	LSDV079	68	D1R	63
80L	68927	68466	153	L	Virion protein	80L	224	69	SPV077	39	M077L	38	LSDV080	33	D2L	42
81R	68926	69663	245	?	Virion protein	81R	332	64	SPV078	31	M078R	28	LSDV081	38	D3R	32
82R	69660	70319	219	?	Uracil DNA glycosylase	82R	394	82	SPV079	69	M079R	71	LSDV082	70	D4R	67
83R	70393	72753	786	L	NTPase, TM	83R	1465	91	SPV080	74	M080R	75	LSDV083	74	D5R	66
84R	72750	74657	635	L	Early transcription factor VETFs, TM	84R	1227	95	SPV081	87	M081R	87	LSDV084	88	D6R	80
85R	74690	75172	160	L	RNA polymerase subunit RPO18	85R	309	94	SPV082	71	M082R	77	LSDV085	78	D7R	73
86R	75194	75859	221	?	*mutT* motif	86R	367	87	SPV083	62	M084R	56	LSDV086	64	D9R	55
87R	75856	76572	239	L	*mutT* motif	87R	431	89	SPV084	60	M085R	61	LSDV087	62	D10	50
88L	78481	76586	631	L	NPH-1, transcription termination factor	88L	1159	90	SPV085	69	M086L	67	LSDV088	71	D11L	69
89L	79373	78510	287	L	mRNA capping enzyme, VITF	89L	528	91	SPV086	78	M087L	73	LSDV089	74	D12L	70
90L	81059	79398	553	L	Rifampin resistance protein	90L	1055	93	SPV087	79	M088L	77	LSDV090	80	D13L	73
91L	81531	81076	151	L	Late transcription factor, VLTF-2	91L	266	86	SPV088	62	M089L	68	LSDV091	64	A1L	62
92L	82229	81555	224	?	Late transcription factor, VLTF-3	92L	442	95	SPV089	83	M090L	86	LSDV092	85	A2L	84
93L	82453	82226	75	L	Unknown	93L	139	84	SPV090	55	M091L	69	LSDV093	63	A2.5L	53
94L	84440	82467	657	L	Virion core protein	94L	1195	90	SPV091	73	M092L	71	LSDV094	70	A3L	63
95L	84946	84500	148	L	Virion core protein	95L	201	70	SPV092	37	M093L	33	LSDV095	37		
96R	84986	85483	165	L	RNA polymerase subunit RPO19	96R	260	80	SPV093	54	M094R	52	LSDV096	56	A5R	58
97L	86595	85480	371	L	Unknown	97L	673	91	SPV094	70	M095L	70	LSDV097	75	A6L	56
98L	88760	86619	713	L?	Early transcription factor, VETF1	98L	1273	89	SPV095	74	M096L	73	LSDV098	74	A7L	68
99R	88817	89692	291	E?	Intermediate transcription factor VITF-3	99R	528	90	SPV096	64	M097R	68	LSDV099	64	A8R	61
100L	89932	89693	79	L	IMV membrane protein, SP, TM	100L	146	91	SPV097	82	M098L	72	LSDV100	74	A9L	71
101L	92641	89933	902	L	Virion core protein P4a	101L	1575	87	SPV098	64	M099L	57	LSDV101	62	A10L	50
102R	92656	93600	314	L	Unknown	102R	521	85	SPV099	72	M100R	69	LSDV102	71	A11R	52
103L	94104	93601	167	L	Virion core protein	103L	249	77	SPV100	55	M101L	61	LSDV103	55	A12L	46
104L	94357	94151	68	L	IMV membrane protein, TM	104L	122	83	SPV101	51	M102L	47	LSDV104	58	A13L	35
105L	94685	94404	93	L	IMV membrane protein SP, TM	105L	160	82	SPV102	72	M103L	64	LSDV105	65	A14L	45
106L	94864	94676	62	L	Virulence factor, SP	106L	46	86	SPV103	76	M104L	81	LSDV106	67		
107L	95138	94854	94	L	Unknown	107L	167	78	SPV104	51	M105L	52	LSDV107	55	A15L	49
108L	96267	95122	381	L	Myristylated membrane protein, TM	108L	629	78	SPV105	58	M106L	54	LSDV108	60	A16L	50

Continued on facing page

TABLE 1—*Continued*

ORF	Codon		No. of aa[f]	TOE[g]	Predicted structure or function[h]	YLDV[a]			SPV[b]		Myx[c]		LSDV[d]		VV[e]	
	Start	Stop				ORF	BLASTP2 score	% Identity	ORF	% Identity	ORF	% Identity	ORF	% Identity	ORF	% Identity
109L	96847	96278	189	L	Phosphorylated IMV membrane protein, TM	109L	299	80	SPV106	59	M107L	51	LSDV109	50	A17L	37
110R	96862	98298	478	?	DNA helicase, TM	110R	839	85	SPV107	61	M108R	62	LSDV110	57	A18R	55
111L	98503	98279	74	L	Unknown	111L	102	68	SPV108	69	M109L	81	LSDV111	75	A19L	58
112L	98840	98508	110	L	TM	112L	167	71	SPV110	49	M110L	44	LSDV113	47	A21L	44
113R	98839	100119	426	?	DNA polymerase processivity factor	113R	668	75	SPV109	48	M111R	46	LSDV112	51	A20R	46
114R	100126	100602	158	L	DNA processing	114R	259	77	SPV111	66	M112R	60	LSDV114	65	A22R	63
115R	100625	101773	382	L	Intermediate transcription factor VITF-3	115R	614	80	SPV112	59	M113R	58	LSDV115	61	A23R	59
116R	101775	105269	1164	L	RNA polymerase subunit RPO132	116R	2179	92	SPV113	84	M114R	83	LSDV116	85	A24R	79
117L	105724	105272	150	L	Fusion protein SP, TM	117L	125	48	SPV114	39	M115L	25	LSDV117	31	A27L	56
118L	106150	105725	141	L		118L	215	70	SPV115	57	M116L	52	LSDV118	57	A28L	48
119L	107065	106163	300	?	RNA polymerase subunit RPO35	119L	528	85	SPV116	64	M117L	62	LSDV119	64	A29L	56
120L	107261	107034	75	L	Virion protein	120L	99	72	SPV117	45	M118L	46	LSDV120	45	A30L	51
120.5L	107421	107287	44	?	Unknown	120.5L			SPV117.5		M119L		LSDV118.5		A30.5L	
121L	108224	107460	254	L	DNA packaging	121L	466	90	SPV118	79	M120L	81	LSDV121	84	A32L	60
122R	108278	108826	182	L?	EEV glycoprotein, TM	122R	208	58	SPV119	30	M121R	36	LSDV122	32	A33R	27
123R	108849	109361	170	L	EEV protein	123R	271	75	SPV120	57	M122R	51	LSDV123	48	A34R	45
124R	109364	109942	192	?	Unknown	124R	266	70	SPV121	40	M123R	43	LSDV124	36	A35R	38
125R	109969	110826	285	I?	TM	125R	436	75	SPV122	36	M124R	39	LSDV125	36		
126R	110872	111366	164	?	EEV glycoprotein, TM	126R	69	29								
127R	111457	112257	266	E/L?	TM	127R	379	70	SPV124	37	M126R	33	LSDV127	37	A37R	26
128L	113060	112260	266	L?	CD47	128L	263	52	SPV125	28	M128L	26	LSDV128	26		
129R	113065	113481	138	L?		129R	202	75			M129R	40			E7R	26
131R	113605	113856	83	L		131R	49	38								
132R	113894	114151	85	E	Unknown	132R	92	59	SPV127	35			LSDV130	40		
135R	114315	120002	1895	L?	8 TM, SP	135R	2805	72	SPV131	56	M134R	52	LSDV134	43		
137R	120468	120932	154	E	A52R family	137R	195	62	SPV133	32	M136R	31	LSDV136	34	C6L	28
138R	120962	121981	339	L	Unknown	138R	453	64	SPV134	36	M137R	31	LSDV137	39	A51R	34
139R	122047	122631	194	?	A52R family	139R	253	68	SPV135	43	M139R	43	(LSDV136)	28	A52R	34
141R	122895	123254	119	E?	Ox-2 mimic	141R	172	72			M141R	38	LSDV138	51		
142R	123296	124225	309	?	Ser/Thr protein kinase	142R	560	84	SPV137	57	M142R	57	LSDV139	59	B1R	47
143R	124262	124972	236	L	Host range RING finger protein	143R	403	80	SPV138	43	M143R	47	LSDV140	40		
144R	125037	125843	268	L	CD46 mimic	144R	283	65	SPV139	48	M144R	37	LSDV141	43	C3L	37
145R	126011	127000	329	?	vCCR8	145R	375	60	SPV146	30			LSDV011	31		
146R	127424	128494	356	?	Ankyrin repeat	146R	534	73	SPV142	35	M149R	33	LSDV147	37	B4R	24
147R	128524	130017	497	?	Ankyrin repeat	147R	727	72	SPV143	28	M148R	26	LSDV148	30	B4R	22
148R	130014	131465	483	?	Ankyrin repeat	148R	588	62	SPV144	25	M149R	24	LSDV152	24	B4R	16
149R	131527	132456	310	E	Serpin/SPI-2 ortholog	149R	490	75	SPV145	37	M151R	40	LSDV149	40	C12L	29
150R	132492	132812	106	L	Unknown	150R	152	74	SPV147	33	M004.1	29	LSDV153	26		
151R	132914	133918	334	E	A52R family	151R	491	72					LSDV007	34	C10L	26

[a] Ortholog from YLDV (accession no. AJ293568).
[b] Ortholog from SPV (accession no. AF410153).
[c] Ortholog from myxoma virus (accession no. AF170726).
[d] Ortholog from LSDV (accession no. AF325528).
[e] Ortholog from vaccinia virus strain Copenhagen (accession no. M35027).
[f] aa, amino acids.
[g] Predicted promoters (early [E], intermediate [I], and late [L]) were determined (15). ?, uncertain or unknown; TOE, time of expression.
[h] Predicted functions were determined by identifying YMTV orthologs from YLDV and SPV. Abbreviations: vTNF-α, viral tumor necrosis factor alpha; SP, signal peptide; TM, transmembrane domain; eIF2α, eukaryotic initiation factor 2α; IL-18, interleukin-18; EEV, extracellular enveloped virions; bp, binding protein. BLASTP2 scores were determined by performing BLAST searches at http://www.ncbi.nlm.nih.gov/BLAST/.

tiple poxviruses. An unusual number of large gaps occur between ORFs in YMTV (Table 1) and YLDV (15). Our assumption is that if these presumptive noncoding regions between yatapox virus ORFs have important functions, then they would likely be conserved between YLDV and YMTV. The largest inter-ORF gap in YLDV is 376 bases and maps between 23L and 24L (15). The corresponding region in YMTV is a 474-bp gap between 22L and 24L, with YMTV

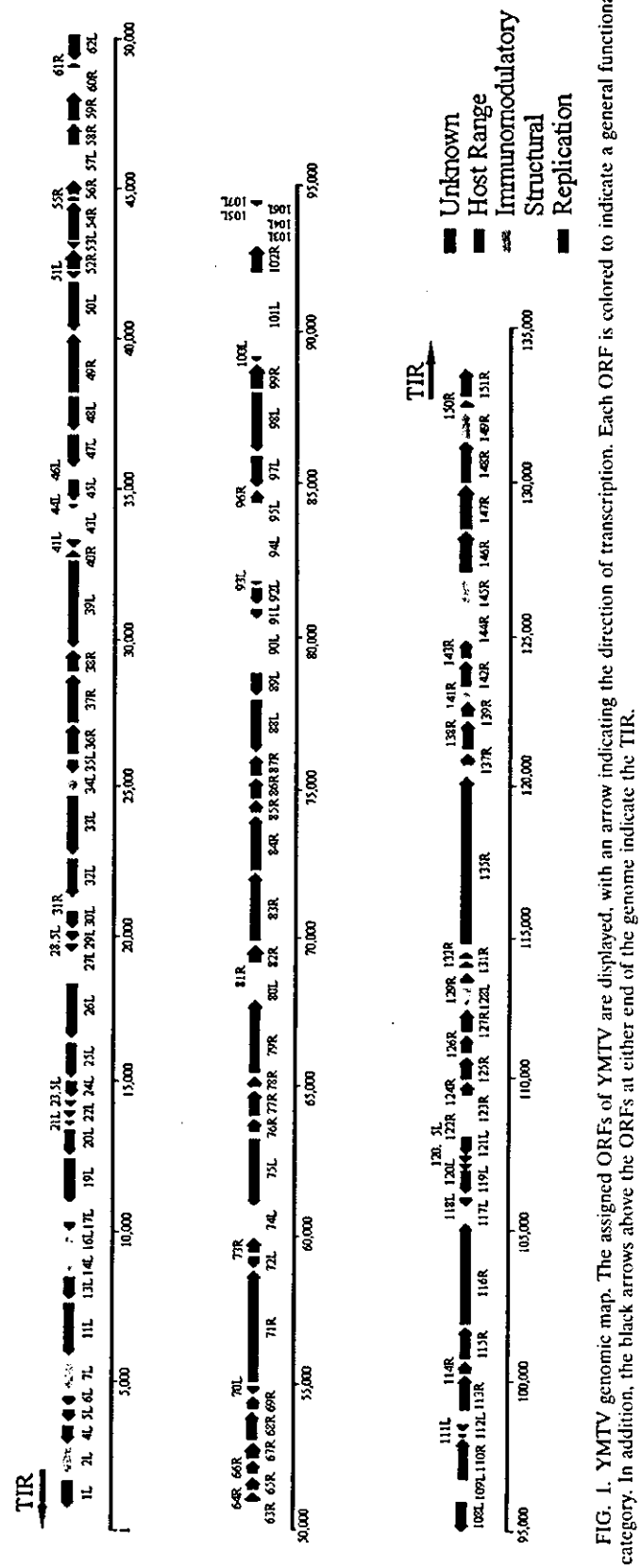

FIG. 1. YMTV genomic map. The assigned ORFs of YMTV are displayed, with an arrow indicating the direction of transcription. Each ORF is colored to indicate a general functional category. In addition, the black arrows above the ORFs at either end of the genome indicate the TIR.

TABLE 2. Immune evasion ORFs and ORFs absent from YMTV but present in YLDV

YMTV ORF	YLDV ORF	Putative function(s)[a]
2L	2L	vTNF bp
	3L	A52R ortholog, TLR signaling inhibitor
7L	7L	vCCR8
	8L	4 ankyrin domains
	9L	Ortholog of vv M2L
	10L	Secreted serpin, myxoma virus SERP-1 ortholog
12L	12L	eIF2α mimic
14L	14L	vIL-18 bp
	15L	EGF domain
16L	16L	Inhibition of apoptosis, ortholog of myxoma virus M11L
	18L	Ortholog of myxoma virus M013L
	23L	Unknown
	28R	Unknown
34L	34L	dsRNA bp
	42L	Ortholog of vv O1L
128L	128L	CD47 mimic
	130L	Unknown
133L	133L	3β-HSD
	134R	vIL-10
	136R	IFN-α/β binding protein
	140R	Ortholog of vv A54R, kelch-like protein
141R	141R	Ox-2 mimic
144R	144R	CD46 mimic
145R	145R	CCR8 mimic
149R	149R	Intracellular serpin, SPI-2 ortholog

[a] Abbreviations: vTNF, viral tumor necrosis factor; vCCR8, viral CCR8 ortholog; vv, vaccinia virus; eIF2α, eukaryotic initiation factor 2α; vIL-18, viral interleukin-18; EGF, epidermal growth factor; dsRNA, double-stranded RNA; vIL-10, viral interleukin-10; IFN-α/β, alpha/beta interferon; bp, binding protein.

lacking any obvious ortholog of 23L. As Table 1 illustrates, a small ORF between 22L and 24L of YMTV was identified and designated 23.5L (Table 1; Fig. 3a). Orthologs of 23.5L were previously reported in myxoma virus, LSDV, and vaccinia virus (8, 13, 29).

Since YMTV23.5L was present in a number of divergent poxvirus species, we wanted to examine whether YLDV and SPV might carry a 23.5L version in their genomes. We examined the large noncoding region between YLDV23L and YLDV24L and identified a 153-bp orthologous ORF, which we have designated 23.5L in YLDV (Fig. 3a). This YLDV ORF was classified as a predicted ORF in the annotated sequence of YLDV (accession no. AJ293568) but was not classified as an authentic ORF in the published sequence (15). Interestingly, an ortholog of YMTV23.5L was also found in SPV between positions 13229 and 13445 on the genomic sequence map (3) that had significant similarity to other versions of 23.5L (Fig. 3b). However, this potential ORF in SPV lacks a canonical start codon (ATG) (Fig. 3b), suggesting that the SPV version is either a pseudogene or a sequencing error that resulted in the insertion of an extra nucleotide between a potential upstream start ATG codon in an alternative reading frame six codons upstream of the assigned codon for the first lysine residue.

Unusual conserved promoter-like sequence found in yatapox, suipox, capripox, and leporipox viruses. The identification of the 212-bp gene YMTV23.5L greatly reduced the amount of assigned noncoding sequence in the region between 22L and 24L. Nevertheless, when we continued our analysis of the noncoding sequence in this region between the ORFs 23.5L and 24L in YMTV and YLDV, we noticed a striking 42-bp sequence that was 100% identical between YMTV and YLDV (Fig. 4a).

To determine whether this sequence was conserved in other poxviruses, we examined the region between the orthologs of 23.5L and 24L in SPV (SPV020.5 and SPV021), LSDV (LSDV023 and LSDV024), myxoma virus (M018L and M019L), and vaccinia virus (F8L and F9L). Figure 4a demonstrates that this identical nucleotide sequence is found in SPV, LSDV, goatpox virus, and sheeppox virus and was 95% conserved in myxoma virus but is not present in vaccinia virus or other orthopoxviruses. The unusually high degree of sequence conservation (i.e., 100% identity between positions 2 through 41 [Fig. 4a] for YMTV, YLDV, SPV, and LSDV) suggests that the sequence may have an important and conserved function.

Analysis of the sequence identified two 9-bp repeats separated by 10 bases (Fig. 4a). Since one turn of the DNA double helix is 10.4 bp, this suggests that the two repeats are registered on the same face of the DNA molecule. One possible function for this type of sequence arrangement is the binding of transcription factors to the DNA sequence, and indeed the sequence does resemble a tandem repeat of a canonical poxvirus late promoter (9). To test whether the conserved sequence might function as a viral promoter element, we inserted the conserved 42-bp sequence (derived from myxoma virus) in

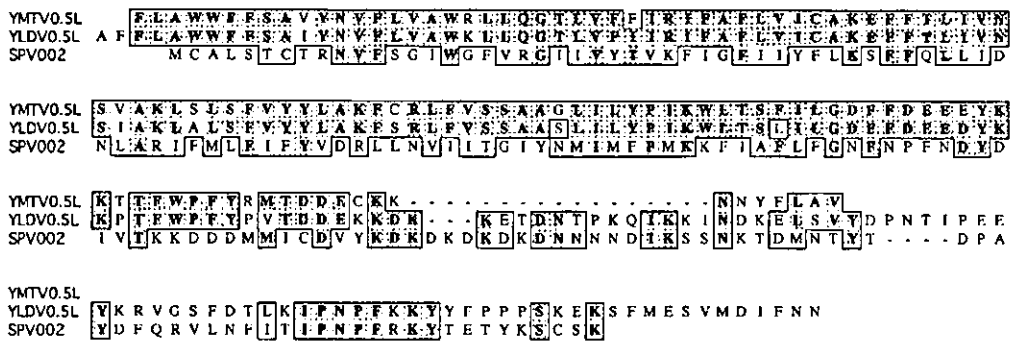

FIG. 2. YMTV and YLDV each contain an apparent pseudogene within the noncoding region of the termini. An alignment of the assigned SPV002 ORF (3) with a portion of the noncoding region of the YMTV and YLDV termini is shown.